eLIFE
elifesciences.org

TOOLS AND RESOURCES

Extensive cargo identification reveals distinct biological roles of the 12 importin pathways

Makoto Kimura[1]*, Yuriko Morinaka[1], Kenichiro Imai[2,3], Shingo Kose[1], Paul Horton[2,3], Naoko Imamoto[1]*

[1]Cellular Dynamics Laboratory, RIKEN, Wako, Japan; [2]Artificial Intelligence Research Center, National Institute of Advanced Industrial Science and Technology, Tokyo, Japan; [3]Biotechnology Research Institute for Drug Discovery, National Institute of Advanced Industrial Science and Technology, Tokyo, Japan

Abstract Vast numbers of proteins are transported into and out of the nuclei by approximately 20 species of importin-β family nucleocytoplasmic transport receptors. However, the significance of the multiple parallel transport pathways that the receptors constitute is poorly understood because only limited numbers of cargo proteins have been reported. Here, we identified cargo proteins specific to the 12 species of human import receptors with a high-throughput method that employs stable isotope labeling with amino acids in cell culture, an in vitro reconstituted transport system, and quantitative mass spectrometry. The identified cargoes illuminated the manner of cargo allocation to the receptors. The redundancies of the receptors vary widely depending on the cargo protein. Cargoes of the same receptor are functionally related to one another, and the predominant protein groups in the cargo cohorts differ among the receptors. Thus, the receptors are linked to distinct biological processes by the nature of their cargoes.
DOI: 10.7554/eLife.21184.001

***For correspondence:** makimura@riken.jp (MK); nimamoto@riken.jp (NI)

Competing interests: The authors declare that no competing interests exist.

Funding: See page 23

Received: 02 September 2016
Accepted: 17 January 2017
Published: 24 January 2017

Reviewing editor: Karsten Weis, ETH Zurich, Switzerland

Introduction

In interphase cells, proteins and RNAs migrate into and out of the nuclei through the central channels of the nuclear pore complexes (NPC) embedded in the nuclear envelope. These nuclear pores are lined with FG-repeat domains that constitute a permeability barrier, and only macromolecules that reversibly interact with the FG-repeats can permeate this barrier (***Schmidt and Görlich, 2016***). One such group of proteins, the importin (Imp)-β family proteins, are nucleocytoplasmic transport receptors (NTRs) that primarily carry nuclear proteins and small RNAs as their cargoes through the nuclear pores, although non-importin family NTRs also act depending on the cargo and physiological conditions (***Kose et al., 2012***; ***Lu et al., 2014***; ***Weberruss et al., 2013***). The human genome encodes 20 species of Imp-β family NTRs, of which 10 [Imp-β, transportin (Trn)-1, -2, -SR (-3), Imp-4, -5 (RanBP5), -7, -8, -9, and -11] are nuclear import receptors, 7 [exportin (Exp)-1 (CRM1), -2 (CAS/CSE1L), -5, -6, -7, -t, and RanBP17] are export receptors, 2 (Imp-13 and Exp-4) are bi-directional receptors, and the function of RanBP6 is undetermined (***Kimura and Imamoto, 2014***). These NTRs constitute multiple parallel transport pathways. The basic mechanism of directional transport was elucidated in the early years (***Görlich and Kutay, 1999***), but even today, the number of NTR-specific cargoes that has been reported is surprisingly small, hindering a biological understanding of the nucleocytoplasmic transport system.

NTRs are thought to transport specific cohorts of cargoes by binding to specific sites on those cargoes (***Chook and Süel, 2011***), but the consensus structures of the NTR-binding sites have been established for only a few NTRs (***Soniat and Chook, 2015***) as follows: the classical nuclear

localization signal (cNLS) for the Imp-α family adapters, which connects Imp-β and cargoes (**Lange et al., 2007**); PY-NLS for Trn-1 and -2 (**Lee et al., 2006**; **Süel et al., 2008**); the nuclear export signal (NES) for Exp-1 (**Hutten and Kehlenbach, 2007**); the SR-rich domain that binds to Trn-SR (**Kataoka et al., 1999**; **Maertens et al., 2014**); and Lys-rich NLS (IK-NLS) for yeast Kap121p (Imp-5 homolog; **Kobayashi and Matsuura, 2013**; **Kobayashi et al., 2015**). The β-like importin-binding (BIB) domain is another NTR-binding site (**Jäkel and Görlich, 1998**), but its consensus sequence and NTR specificity remain obscure. Among the NTRs, Imp-β exclusively uses one of the seven species of the Imp-α family of proteins as an adapter for cargo binding, and many Imp-α/β cargoes have been reported, although Imp-β also directly binds to cargoes (**Goldfarb et al., 2004**). Among the import receptors, Trn-1 and its closest homolog Trn-2 have the second-highest number of cargoes reported thus far, and the PY-NLS motif has been defined, although in some cases the motif is difficult to recognize because of sequence diversity and structural disorder is another requisite (**Soniat and Chook, 2015**, **2016**). For the cargoes of other NTRs, the consensus structures of NTR-binding sites have hardly been derived because only limited numbers of cargoes have been reported, including Imp-β-direct cargoes.

There are many reports on the differential spatiotemporal expression of Imp-β family NTRs, including tissue specificities in humans (**Quan et al., 2008**), developmental or spermatogenic stage specificities in mice (**Major et al., 2011**; **Quan et al., 2008**), and tissue or response specificities in plants (**Huang et al., 2010**). Expression regulation is not only transcriptional but also miRNA-mediated (**Li et al., 2013**; **Szczyrba et al., 2013**) or locally translationally mediated (**Perry and Fainzilber, 2009**). Additionally, the NTRs are functionally regulated by protein modifications (**Wang et al., 2009**), inhibitory factors (**Lieu et al., 2014**), and specific anchorings (**Makhnevych et al., 2003**). These nucleocytoplasmic transport regulations must significantly influence cellular physiology, and their significance may be elucidated if the affected cargoes can be specified. Indeed, in previous studies, NTR regulations have been linked to cellular responses through the functions of specific cargoes. For example, in prostate cancer cells treated with a cinnamaldehyde derivative, the expression of Imp-7 and the transcription factor Egr1 are induced, and the Egr1 imported by Imp-7 activates apoptotic gene transcription (**Kang et al., 2013**). In another example, when the nuclear import of some ribosomal proteins (RPs) is inhibited by the repression of Imp-7 expression, other unassembled RPs restrain the negative regulator of p53 Mdm2 and thereby activate p53 to inhibit cell growth (**Golomb et al., 2012**). Additionally, the inhibition of Trn-2 by the caspase-generated HuR (ELAVL1) fragment is crucial for the cytoplasmic retention of full-length HuR, which induces myogenesis (**Beauchamp et al., 2010**) or staurosporine-induced apoptosis (**von Roretz et al., 2011**). In many other studies, mutations of particular NTR genes in model organisms, including yeast, flies, and plants, have resulted in defects in specific biological processes (**Kimura and Imamoto, 2014**). Thus, each NTR has its own inherent biological significance. However, the details of the molecular processes are largely uncharacterized because the responsible cargoes have not been identified. If we could identify more cargoes, further studies of cellular regulation by nucleocytoplasmic transport would be possible.

We previously established a method for identifying the cargoes of a nuclear import receptor called SILAC-Tp (**Kimura et al., 2013a**, **2013b**, **2014**). SILAC-Tp employs stable isotope labeling with amino acids in cell culture (SILAC) (**Ong et al., 2002**), an in vitro reconstituted nuclear transport system (**Adam et al., 1990**), and quantitative mass spectrometry. A recent advancement of the Orbitrap mass spectrometer drastically increased the identified and quantified protein numbers, and this advancement has been successfully applied to other cargo identification methods (**Kırlı et al., 2015**; **Thakar et al., 2013**). Here, we utilized this advancement for the SILAC-Tp method and identified import cargoes of all 12 NTRs, of which 10 are import and two are bi-directional receptors. Our results illustrate the basic framework and the biological significance of the nucleocytoplasmic transport pathways.

Results and discussion

SILAC-Tp effectively identifies cargoes

SILAC-Tp employs an in vitro nuclear transport system, and all 12 NTRs import their reported specific cargoes in this system (**Figure 1—figure supplement 1C**). The transport system consists of

permeabilized HeLa cells labeled with 'heavy' amino acids by SILAC, unlabeled HeLa nuclear extract depleted of Imp-β family NTRs and RCC1, unlabeled HeLa cytosolic extract depleted of Imp-β family NTRs, one species of recombinant NTR, p10/NTF2, and an ATP regeneration system. Unlabeled 'light' proteins in the nuclear extract are imported into the nuclei of the permeabilized cells. Simultaneously, a control reaction without the NTR is performed. Next, the proteins are extracted from the nuclei and identified and quantified by LC-MS/MS. The recipient nuclei contain both the imported and endogenous proteins, and the ratio of the imported to the endogenous fraction of a protein is calculated as the unlabeled/labeled or light/heavy (L/H) ratio. The quotient of the L/H ratios with the NTR (+NTR) and without it (control), that is, $(L/H_{+NTR})/(L/H_{Ctl})$, of a protein is defined as the +NTR/Ctl value and is used as the index for cargo potentiality.

In one run of SILAC-Tp (control or +NTR), approximately 2500 to 4000 proteins were identified, and the L/H ratios of 1700 to 3100 proteins were quantified. To calculate the +NTR/Ctl value, one protein has to be quantified in both the control and +NTR reactions, and we discarded L/H_{+NTR} values that lacked the counterpart L/H_{Ctl} values. We performed three replicates of SILAC-Tp for each of the 12 NTRs. In the three replicates, 1235 to 1671 proteins were assigned with +NTR/Ctl values three times, and 364 to 502 proteins were assigned only twice (***Supplementary file 1***). We did not consider proteins with single +NTR/Ctl values, although a protein with only a single but high +NTR/Ctl value may still be a cargo (see below). To normalize the index values of the three replicates, the Z-scores of the $\log_2$(+NTR/Ctl) were calculated within each replicate (***Figure 1—figure supplement 2A and B***). Ranking the proteins that have three +NTR/Ctl values by the median of the three Z-scores may reasonably sort the candidate cargoes. However, if the lower Z-score of a protein with only two +NTR/Ctl values is higher than the median Z-scores of those candidate cargoes, the protein may also be a candidate cargo. Thus, we ranked the proteins by the second (the lower of the two or the middle of the three) Z-scores, and termed the result the 2nd-Z-ranking (***Supplementary file 1***).

To define the border that separates candidate cargoes from other proteins in the 2nd-Z-ranking, we first reviewed the distribution of reported Trn-1 cargoes in the Trn-1 2nd-Z-ranking because many Trn-1 cargoes have been reported. For an unbiased evaluation, we employed the lists of cargoes consolidated by other researchers (***Chook and Süel, 2011***). Twenty-seven reported cargoes were included in the 2nd-Z-ranking (totaling 1649 proteins; ***Supplementary file 1***, Trn-1 'Report and feature'). We calculated the reported cargo rates (to serve as a proxy for precision), recall, and Fisher's exact test p-values for rank cutoffs in increments of 1%. Computing reported cargo rate requires deciding which candidate cargoes should be considered as false positives. Since a gold standard set of definitely non-cargo proteins is not available, it is not clear which previously unreported cargoes should be counted as false positives, and which, if any, should be discarded as unclear. Therefore, we estimated reported cargo rates in two ways: (i) treating all the 1622 proteins not reported as cargoes as negative examples (***Figure 1—figure supplement 3A*** and ***Figure 1—source data 1A***); and (ii) discarding proteins with undetermined or nuclear subcellular localization according to Uniprot annotation, and treating the remaining 259 non-nuclear proteins as negative examples (***Figure 1—figure supplement 3A*** and ***Figure 1—source data 1B***). In the former case, the reported cargo rate corresponds to a lower bound on the precision, and even in the latter case, the reported cargo rates are expected to underestimate precision, because almost certainly some of the proteins that we exclude as unclear are in fact true cargoes.

To select cargoes with high sensitivity, we employed the cutoff of 15% that yields a high recall of 0.741 (***Figure 1—figure supplement 3B*** and ***Figure 1—source data 1A and 1B***; recall is not affected by the assumptions of negative examples). Among the 27 reported cargoes, 20 cargoes were ranked in the top 15% (247 proteins; $p=5.39 \times 10^{-12}$ by Fisher's exact test), and the others were dispersed in the lower ranks (***Figures 1A*** and ***2A***; ***Figure 1—figure supplement 2C and E***).

We examined the direct binding of Trn-1 to a subset of proteins in the 2nd-Z-ranking using a bead halo assay (***Patel and Rexach, 2008***) (***Supplementary file 2***) in which the binding of GFP-fusion proteins to GST-Trn-1 on glutathione-Sepharose beads was observed by fluorescence microscopy. If RanGTP (a Q69L GTP-fixed mutant) (***Bischoff and Ponstingl, 1995***) inhibits the protein–Trn-1 binding, the functionality of the binding is verified. For all the bead halo assays in this work, we principally selected well-characterized proteins that have not been reported as cargoes from (i) proteins ranked high (within the top 15% in the 2nd-Z-ranking or 4% in the 3rd-Z-ranking, see below), around presumptive cutoffs (within about top 15–25% in the 2nd-Z-ranking), or lower and (ii) highly ranked proteins that are suspected as indirect cargoes or false positives based on their well-known

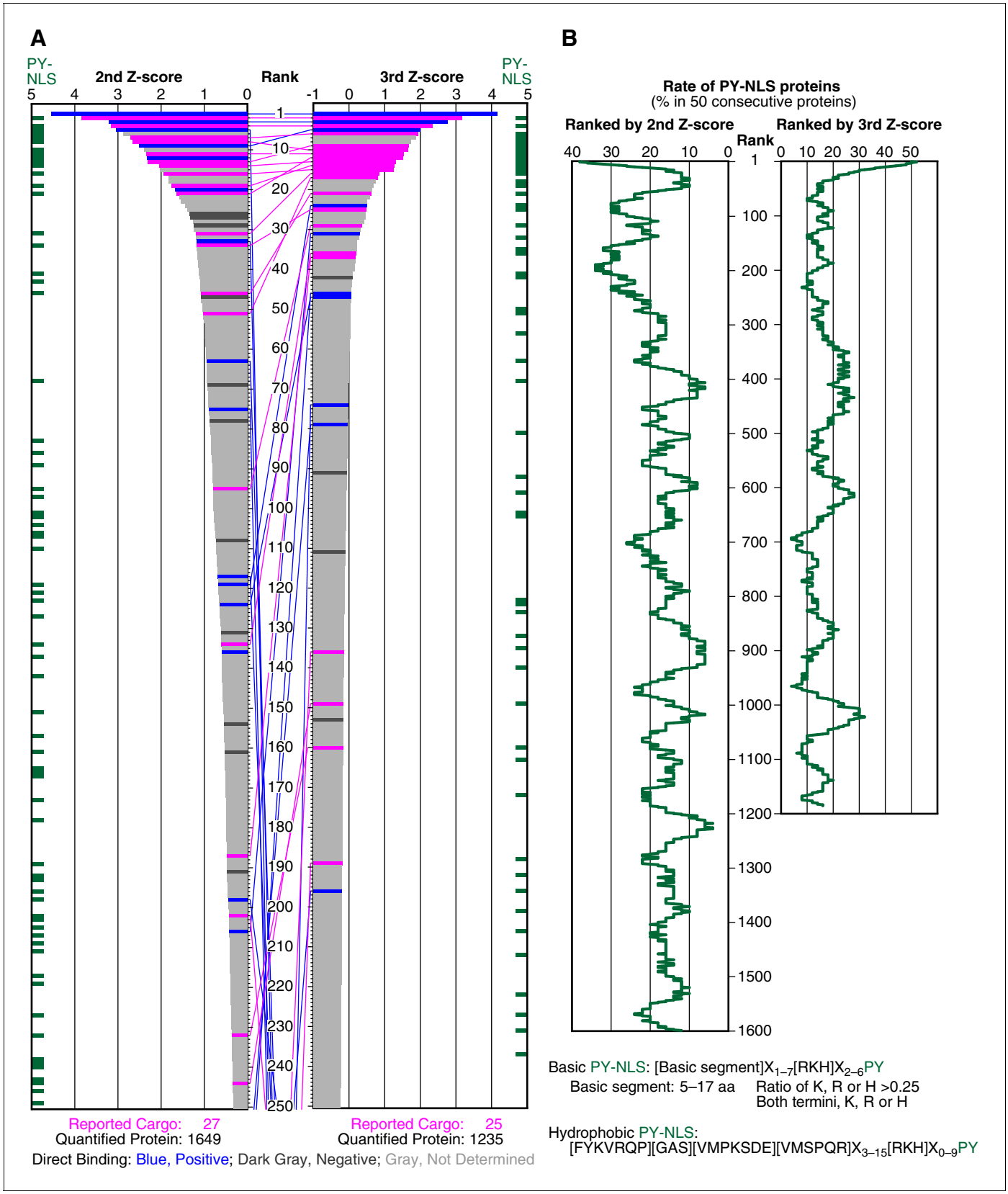

Figure 1. SILAC-Tp effectively sorts Trn-1 cargoes. (**A**) Z-scores in the Trn-1 2nd- and 3rd-Z-rankings. The second (left) and third (right) Z-scores are presented for the top 250 proteins in the Trn-1 2nd- and 3rd-Z-rankings, respectively. The total number of ranked (quantified) proteins and the number

Figure 1 continued on next page

Figure 1 continued

of previously reported cargoes included in the ranking are indicated at the bottom. The magenta bars represent previously reported cargoes. The blue and dark gray bars represent the proteins that did and did not bind directly to Trn-1, respectively, in the bead halo assays (***Supplementary file 2***). Identical proteins marked by the colors are connected by lines. Proteins that carry PY-NLS motifs are indicated by green bars. (**B**) Distribution of PY-NLS motif-containing proteins in the rankings. The percentage of the proteins carrying PY-NLS motifs in 50 consecutively aligned proteins is presented along with the 2nd- and 3rd-Z-rankings (left and right, respectively). For example, the top 50 proteins in the 2nd-Z-ranking include 19 (38%) PY-NLS motif-containing proteins, and thus the value at position 1 is 38%. Two types of PY-NLS motifs, basic and hydrophobic, are defined as presented at the bottom.

DOI: 10.7554/eLife.21184.002

The following source data and figure supplements are available for figure 1:

Source data 1. Statistical analysis of reported cargoes in the Trn-1 2nd- and 3rd-Z-ranking.

DOI: 10.7554/eLife.21184.003

Figure supplement 1. SILAC-Tp experimental system.

DOI: 10.7554/eLife.21184.004

Figure supplement 2. Trn-1 cargoes are effectively sorted by the second or third Z-scores in three replicates of SILAC-Tp.

DOI: 10.7554/eLife.21184.005

Figure supplement 3. Reported cargo rates and recall of the Trn-1 2nd- and 3rd-Z-ranking.

DOI: 10.7554/eLife.21184.006

features, for example, S100A6 or EEF1A2 (see the legend of ***Supplementary file 2***). The negative rate of the bead halo assays should be higher than the true overall false-positive rate of the SILAC-Tp, because proteins in (ii) are selected preferentially. Seventeen novel candidate cargoes in the top 266 (top 16%) bound to Trn-1, and RanGTP inhibited the binding (***Figure 1A***; ***Supplementary file 1***, Trn-1 'Direct binding'; ***Supplementary file 2***). Although the assays were not comprehensive, many of the highly ranked proteins are *bona fide* Trn-1 cargoes. The highly ranked proteins that did not bind to Trn-1 in the assays are still candidate indirect cargoes that may form complexes with other proteins that directly bind to Trn-1 (see the case of POLE3 for Imp-13 below). As an example of a protein with only a single but high Z-score (+NTR/Ctl value), DIMT1 bound to Trn-1 (DHRS4 with Imp-β is another example), but we did not consider such proteins.

Because many reported Trn-1 cargoes carry PY-NLSs, we examined the distribution of PY-NLS motif-containing proteins in the 2nd-Z-ranking (***Figure 1B***). The percentages of PY-NLS motif-containing proteins within a window width of 50 positions were higher in the range of the top 200, indicating a higher rate of PY-NLS motif-containing proteins within the top 250 (top 15%). The reported Trn-1 cargoes were similarly distributed in the Trn-2 2nd-Z-ranking (***Supplementary file 1***, Trn-2 'Report or feature'). Because Trn-1 and -2 share nearly the same reported cargoes (***Twyffels et al., 2014***), this result demonstrates the reproducibility of the SILAC-Tp method. Based on these evaluations, we assumed that the proteins in the top 15% (247 proteins) of the 2nd-Z-ranking are candidate cargoes with high sensitivity (0.741) and termed them the 2nd-Z-15% cargoes.

Next, we examined whether the cutoff employed for Trn-1 is applicable to Imp-13 and Trn-SR whose 2nd-Z-rankings include several reported cargoes. The Imp-13 2nd-Z-ranking (totaling 2060 proteins) includes eight reported cargoes (***Supplementary file 1***, Imp-13), and seven of these are ranked in the top 244 (top 12%; $p=2.83 \times 10^{-7}$; ***Figure 2B***; ***Figure 2—figure supplements 1A*** and ***2A***). In bead halo assays for a subset of the ranked proteins, 24 novel candidate cargoes in the top 326 (top 16%) bound directly to Imp-13, and RanGTP inhibited the binding (***Figure 2—figure supplement 2A***; ***Supplementary file 1***, Imp-13; ***Supplementary file 2***). One component of a reported cargo complex, that is, POLE3, did not bind to Imp-13, but its binding partner CHRAC1 (***Walker et al., 2009***) did. Thus, the binding partners of the direct cargoes are also ranked high. Many reported Trn-SR cargoes are SR-domain proteins (***Chook and Süel, 2011***), and they can be grouped into either SR-rich splicing factors (SFs) or other SR-domain proteins. The Trn-SR 2nd-Z-ranking (totaling 2021 proteins) contains three reported cargoes (***Supplementary file 1***, Trn-SR), and they are ranked in the top 55 (top 3%; $p=1.91 \times 10^{-5}$; ***Figure 2C***; ***Figure 2—figure supplement 2B***). The 2nd-Z-ranking contains seven SR-rich SFs other than the reported SFs, and five of these are ranked in the top 90 (top 4%; $p=7.61 \times 10^{-18}$). The 2nd-Z-ranking also contains another four proteins that are annotated with 'RS-domain' in UniProt, and three of these are ranked in the top 202 (top 10%; $p=3.65 \times 10^{-3}$). Finally, in bead halo assays for a subset, 11 novel candidate cargoes in

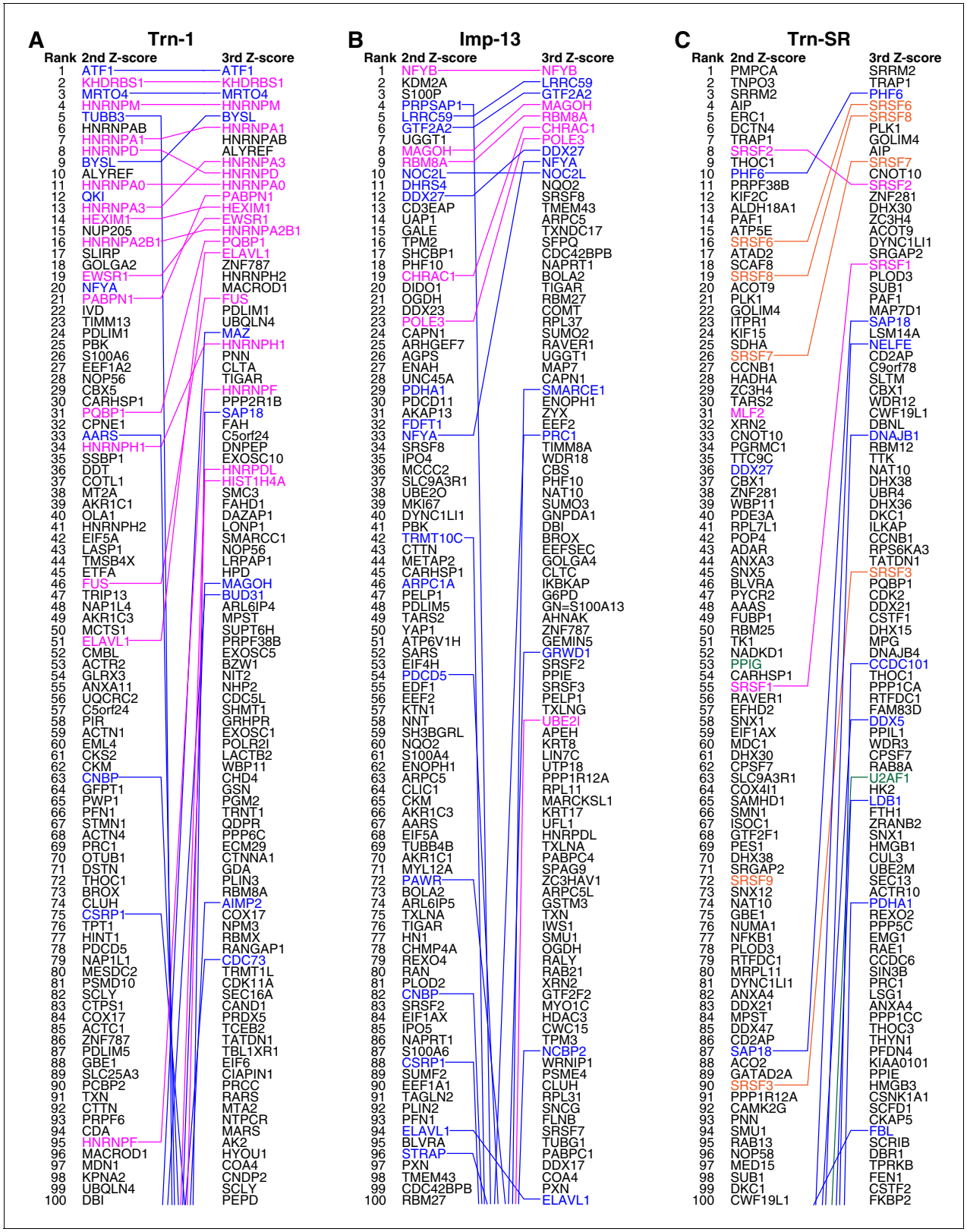

Figure 2. Trn-1, Imp-13, and Trn-SR cargo rankings. (**A**–**C**) The top 100 proteins in the Trn-1 (**A**), Imp-13 (**B**), and Trn-SR (**C**) 2nd- and 3rd-Z-rankings (left and right, respectively). Magenta, reported cargoes; blue, proteins bound directly to the NTR in the bead halo assays (***Supplementary file 2***); orange in (**C**), SR-rich SFs that have not been reported; and green in (**C**), other RS (SR)-domain proteins. Identical proteins marked by the colors are connected by lines.

Figure 2 continued on next page

Figure 2 continued

DOI: 10.7554/eLife.21184.007

The following figure supplements are available for figure 2:

Figure supplement 1. Imp-13 cargoes are effectively sorted by the second or third Z-scores in three replicates of SILAC-Tp.

DOI: 10.7554/eLife.21184.008

Figure supplement 2. SILAC-Tp effectively sorts Imp-13 and Trn-SR cargoes.

DOI: 10.7554/eLife.21184.009

Figure supplement 3. Imp-β cargo ranking and Z-scores in the 2nd- and 3rd-Z-rankings.

DOI: 10.7554/eLife.21184.010

the top 237 (top 12%) bound directly to Trn-SR, and RanGTP inhibited the binding (***Figure 2—figure supplement 2B***; ***Supplementary file 1***, Trn-SR; ***Supplementary file 2***). Hence, the 2nd-Z-15% cargoes could also be defined for Imp-13 (309 proteins) and Trn-SR (302 proteins), and we applied this cutoff to the other NTRs that have few reported cargoes. The 2nd-Z-15% cargoes of the 12 NTRs are presented in ***Supplementary file 3***. Some of the 2nd-Z-15% cargoes with low numbers of L/H counts showed deviation in Z-scores or L/H ratios in the three replicates of SILAC-Tp (***Supplementary file 1***), and an example of their quantitation qualities is presented in ***Supplementary file 4***.

Exceptionally, Imp-β uses Imp-α as an adaptor for cargo binding, and the cytosolic extract used for the transport system contained endogenous Imp-α. Four Imp-αs were found in the Imp-β 2nd-Z-ranking (totaling 2027 proteins), and three of these are in the 2nd-Z-15% cargoes ($p=1.19 \times 10^{-2}$; ***Supplementary file 1***, Imp-β; ***Supplementary file 3***). Thus, the Imp-β candidate cargoes must include both Imp-β-direct and Imp-α-dependent cargoes. Indeed, 31 proteins in the top 276 (top 14%) bound directly to Imp-α, -β, or both in the bead halo assays (***Supplementary file 1***, Imp-β; ***Figure 2—figure supplement 3***; ***Supplementary file 2***). The border for the Imp-β candidate cargoes can be relaxed because Imp-β imports more cargoes than other NTRs with the help of Imp-α. Indeed, in the bead halo assays, many proteins in the top 35% of the 2nd-Z-ranking bound to Imp-α, although most of the proteins that bound directly to Imp-β were ranked in the top 259 (13%). Here, we employed the Imp-β 2nd-Z-15% cargoes (303 proteins) to enable equal comparisons with the cargoes of other NTRs.

Cargo selection with higher specificity

Deviation of the LC-MS/MS quantification within the three replicates complicates cargo selection. However, the Z-scores of the highly ranked reported cargoes were reasonably high in all the three replicates possibly because many of the reported cargoes are abundant proteins that seldom produce outliers in quantification (***Figure 1—figure supplement 2***; ***Figure 2—figure supplement 1***). To select proteins that have high Z-scores in all the three replicates, we next ranked the proteins that had three +NTR/Ctl values by the third (lowest) Z-scores (3rd-Z-ranking). The reported cargo rates, recall, and p-values were calculated in 1% rank increments under two assumptions similarly to the case of 2nd-Z-ranking (***Figure 1—figure supplement 3A and B*** and ***Figure 1—source data 1C and 1D***). The reported cargo rate calculated under the assumption that proteins annotated with non-nuclear localization (178 proteins) are negative examples is as high as 0.85 at the cutoff of top 4% (***Figure 1—figure supplement 3A*** and ***Figure 1—source data 1D***). The Trn-1 3rd-Z-ranking (totaling 1235 proteins) included 25 reported cargoes, and 17 of these were ranked in the top 37 (top 3%; $p=1.67 \times 10^{-22}$; ***Figures 1A*** and ***2A***; ***Figure 1—figure supplement 2D and F***; ***Supplementary file 1***). Seven proteins in the top 47 (top 4%) were novel Trn-1-direct cargoes that were verified in the bead halo assays (***Figures 1A*** and ***2A***; ***Supplementary files 1*** and ***2***). The percentage of PY-NLS motif-containing proteins within a window width of 50 positions was highest at the first position (***Figure 1B***), indicating that PY-NLS motif-containing proteins are concentrated in the top 50 (top 4%). Thus, most of the proteins that ranked in the top 4% (49 proteins) of the 3rd-Z-ranking are highly reliable cargoes, and we termed these proteins the 3rd-Z-4% cargoes. In a comparison between the Trn-1 2nd-Z-15% and 3rd-Z-4% cargoes, most of the 3rd-Z-4% cargoes were also 2nd-Z-15% cargoes (***Figure 1A***). Some reported or newly identified cargoes in the 2nd-Z-15% cargoes were ranked lower in the 3rd-Z-ranking due to the deviations in the third Z-scores.

In the Imp-13 3rd-Z-ranking (totaling 1671 proteins), seven proteins were reported cargoes, and six of these were ranked in the top 58 (top 3%; $p=9.20 \times 10^{-9}$; ***Figure 2B***; ***Figure 2—figure supplements 1B*** and ***2A***; ***Supplementary file 1***). Additionally, the 3rd-Z-4% cargoes (66 proteins) included eight novel cargoes that directly bound to Imp-13 (***Figure 2B***; ***Figure 2—figure supplement 2A***; ***Supplementary files 1*** and ***2***). In the Trn-SR 3rd-Z-ranking (totaling 1591 proteins), both of the two reported cargoes were ranked in the top 18 (top 1%; $p=1.21 \times 10^{-4}$), four of the five other SR-rich SFs were in the top 45 (top 3%; $p=2.74 \times 10^{-6}$), one of the three SR-domain proteins (other than the SR-rich SFs) was ranked 63rd (top 4%; p=0.11), and six novel cargoes within the top 4% (63 proteins) bound directly to Trn-SR (***Figure 2C***; ***Figure 2—figure supplement 2B***; ***Supplementary files 1*** and ***2***). In cases of both Imp-13 and Trn-SR, the proteins were replaced between the 2nd- and 3rd-Z-rankings in a manner similar to the case for Trn-1. We concluded that the 3rd-Z-4% criteria is highly specific including few false positives, albeit at the cost of losing many genuine cargoes. Hence, we employed the 3rd-Z-4% cargoes mainly for the characterization of the identified cargoes, whereas the 2nd-Z-ranking was used for the evaluation of the import efficiencies of the expected cargoes. The 3rd-Z-4% cargoes of the 12 NTRs are presented in ***Figure 3***.

Redundancy in the import pathways

A total of 468 proteins were identified as 3rd-Z-4% cargoes of the 12 NTRs, and 332 of these are unique to one NTR, which clearly reflects the division of roles among the NTRs (***Supplementary file 5B***). Another 136 proteins were shared by two to seven NTRs, and the mean number of shared cargoes between two NTRs was 4.8. In the maximum-likelihood phylogenetic tree of the 12 NTRs (***Figure 4A***), Trn-1 and -2 (84% sequence identity) are paired most closely, and Imp-7 and -8 (65% identity) are the second-most closely paired. These paired NTRs share 28 and 19 cargoes, respectively, and they are paired similarly in a hierarchical clustering based on the cargo profiles (***Figure 4B and C***). The other NTRs that were paired weakly in the phylogenetic tree, namely, Imp-13 and Trn-SR (23% identity), Imp-4 and -5 (22% identity), and Imp-9 and -11 (19% identity), did not form the same pairs when clustering by their cargoes. Thus, the NTR–cargo interactions are conserved only within the highly homologous NTRs. The 2nd-Z-15% cargoes included as many as 1416 proteins in total, 827 of which are shared by two to 12 NTRs, and 589 are unique to one NTR (***Supplementary file 5A and 5D***). Imp-7 and -8 share the largest number (162) among the 2nd-Z-15% cargoes, but Trn-1 and -2 share no more than the other pairs. Of the 247 Trn-1 and 246 Trn-2 2nd-Z-15% cargoes, 69 are shared, and 36 of these are ranked within the top 50 in either ranking. Thus, Trn-1 and -2 still share many highly ranked cargoes but few lower ranked cargoes within the top 15%. The import efficiency of a cargo may differ between Trn-1 and -2, and only one of Trn-1 or -2 may import inefficient cargoes that are ranked lower.

Division of roles among the NTRs

Because NTR-dependent transport is regulated, a cargo cohort of an NTR must be imported simultaneously and act cooperatively. To explore the roles of the NTR cargoes, the 3rd-Z-4% and 2nd-Z-15% cargoes of each NTR were analyzed for enrichment of Gene Ontology (GO) terms (***Gene Ontology Consortium, 2015***) using g:Profiler (***Reimand et al., 2016***). For all the combinations of a GO term and an NTR, the number of cargoes annotated with the term and the significance (p-values according to g:SCS) of the term enrichment are listed (***Supplementary files 6B, 6C***, ***7,*** and ***8***). Depending on the hierarchy of the GO terms, the terms are significantly annotated ($p<0.05$) to the cargo cohorts of none to 12 of the NTRs. Broader terms with smaller term depths are linked to more NTRs, whereas more defined terms with larger term depths are linked to fewer NTRs. Indeed, all 12 of the NTRs are linked to many broad terms, although the cargo numbers and the significances vary widely. Because similar terms were listed redundantly, we selected representative GO terms from those enriched significantly ($p<0.05$) for the 3rd-Z-4% cargoes of the 12 NTRs and tabulated the correspondences between the cargoes and the annotated terms (***Supplementary file 9***). To compare the GO terms that are specifically linked to each NTR, we listed the terms that are enriched significantly for the cargoes of four or fewer NTRs (***Figures 5*** and ***6***). Here, again we extracted the representative terms to decrease the size of the list. The selected terms for the 3rd-Z-4% cargoes plainly exhibit the roles of the cargo cohorts. For example, significant numbers of Imp-4, -7 and Exp-4 cargoes are annotated with DNA recombination or DNA conformation (geometric) change

Imp-β

Z-score Rank 3rd	Z-score Rank 2nd	Gene Name
1	1	KPNB1
2	2	RNMT
3	3	RAM103A1
4	4	KIFC1
5	5	TSR1
6	20	LRRC59
7	19	NCBP2
8	25	NCBP1
9	27	ALKBH5
10	21	NUP214
11	37	SRRT
12	30	NUP88
13	35	GTF2F1
14	22	HELLS
15	53	API5
16	58	CHD8
17	70	POLD3
18	46	RCC1
19	45	ZNF787
20	23	MYOF
21	33	MTA1
22	82	SHMT2
23	84	ALYREF
24	61	GTF2F2
25	94	CTCF
26	73	NOP9
27	67	ZNF24
28	95	PMS2
29	60	WDHD1
30	109	MAZ
31	66	LDB1
32	127	MNAT1
33	144	ZNF146
34	100	TPX2
35	26	OGDH
36	149	CCDC86
37	128	POLR3C
38	119	THYN1
39	97	SMARCE1
40	80	POLD2
41	48	CYR61
42	155	SPIN1
43	121	CCDC58
44	180	HMGA1
45	130	LMNA
46	86	SLTM
47	173	U2SURP
48	185	TCERG1
49	189	PES1
50	145	HNRPLL
51	81	KPNA2
52	188	HMGN3
53	57	RBM27
54	29	KHSRP
55	191	SUMF2
56	222	HNRPDL
57	225	TAF15
58	263	DKC1
59	141	HNRNPUL2
60	219	C9orf78
61	79	MRGBP
62	123	HNRNPU
63	75	OAT
64	168	ATP5A1

Trn-1

Z-score Rank 3rd	Z-score Rank 2nd	Gene Name
1	1	ATF1
2	2	KHDRBS1
3	3	MRTO4
4	4	HNRNPM
5	9	IBYSL
6	7	HNRNPA1
7	6	HNRNPAB
8	10	ALYREF
9	13	HNRNPA3
10	8	HNRNPD
11	11	HNRNPA0
12	21	PABPN1
13	14	HEXIM1
14	19	EWSR1
15	16	HNRNPA2B1
16	31	PQBP1
17	51	ELAVL1
18	86	ZNF787
19	41	HNRNPH2
20	96	MACROD1
21	46	FUS
22	24	PDLIM1
23	99	UBQLN4
24	119	MAZ
25	34	HNRNPH1
26	162	PNN
27	122	CLTA
28	195	TIGAR
29	95	HNRNPF
30	182	PPP2R1B
31	206	SAP18
32	279	FAH
33	57	C5orf24
34	319	DNPEP
35	192	EXOSC10
36	134	HNRPDL
37	187	HIST1H4A
38	147	SMC3
39	331	FAHD1
40	233	DAZAP1
41	276	LONP1
42	378	SMARCC1
43	28	NOP56
44	116	LRPAP1
45	499	HPD
46	388	MAGOH
47	124	BUD31
48	321	ARL6IP4
49	376	MPST

Trn-2

Z-score Rank 3rd	Z-score Rank 2nd	Gene Name
1	1	ATF1
2	10	ETFA
3	4	KHDRBS1
4	5	HNRNPM
5	9	MRTO4
6	7	HNRNPA1
7	14	HNRNPA3
8	13	HNRNPA0
9	16	ALYREF
10	12	HNRNPAB
11	22	PABPN1
12	8	HNRNPD
13	23	EWSR1
14	34	DECR1
15	19	HNRNPA2B1
16	69	UBTF
17	42	HNRNPH2
18	43	FUS
19	29	HEXIM1
20	31	PQBP1
21	37	ELAVL1
22	30	NOP56
23	40	HNRNPH1
24	91	CTR9
25	123	ATP2A2
26	28	PRPF6
27	17	UTP18
28	52	HNRNPF
29	45	APRT
30	206	ARL6IP4
31	185	USP39
32	50	C5orf24
33	65	MAZ
34	300	SAP18
35	105	BUD31
36	228	DAZAP1
37	416	RPL32
38	450	RPL22
39	383	ATL3
40	239	RAB9A
41	217	RAB7A
42	272	LACTB2
43	287	CTNND1
44	144	ZYX
45	425	PRRC2A
46	85	HNRNPH3
47	491	RPL11
48	417	RPL23A
49	141	PNN
50	255	ACSL4

Trn-SR

Z-score Rank 3rd	Z-score Rank 2nd	Gene Name
1	3	SRRM2
2	7	TRAP1
3	10	PHF5
4	16	SRSF6
5	19	SRSF8
6	21	PLK1
7	22	GOLIM4
8	4	AIP
9	26	SRSF7
10	33	CNOT10
11	8	SRSF2
12	38	ZNF281
13	61	DHX30
14	29	ZC3H4
15	20	ACOT9
16	81	DYNC1LI1
17	71	SRGAP2
18	55	SRSF1
19	78	PLOD3
20	98	SUB1
21	14	PAF1
22	130	MAP7D1
23	87	SAP18
24	118	LSM14A
25	123	NELFE
26	86	CD2AP
27	141	C9orf78
28	101	SLTM
29	37	CBX1
30	223	WDR12
31	100	CWF19L1
32	204	DBNL
33	198	DNAJB1
34	159	RBM12
35	180	TTK
36	74	NAT10
37	70	DHX38
38	108	UBR4
39	295	DHX36
40	99	DKC1
41	219	ILKAP
42	27	CCNB1
43	177	RPS6KA3
44	235	TATDN1
45	90	SRSF3
46	150	PQBP1
47	353	CDK2
48	83	DDX21
49	384	CSTF1
50	406	DHX15
51	161	MPG
52	336	DNAJB4
53	416	CCDC101
54	9	THOC1
55	318	PPP1CA
56	79	RTFDC1
57	275	FAM83D
58	116	DDX5
59	466	PPIL1
60	266	WDR3
61	62	CPSF7
62	320	RAB8A
63	202	U2AF1

Imp-4

Z-score Rank 3rd	Z-score Rank 2nd	Gene Name
1	2	IPO4
2	8	PFKL
3	10	BMS1
4	3	TFRC
5	18	MFAP1
6	25	ALPP
7	32	FKBP10
8	55	NELFE
9	17	RBMX
10	31	SFPQ
11	90	CALU
12	19	SLTM
13	88	ESYT1
14	115	HNRNPUL2
15	42	PLK1
16	89	CMAS
17	12	PICALM
18	119	RCC1
19	101	PRCC
20	13	BCLAF1
21	111	PPIL3
22	67	HSPA9
23	129	DHX9
24	130	HMGB1
25	131	FTH1
26	165	RAB7A
27	71	CHCHD2P9
28	147	DNAJC8
29	211	RPL36AL
30	92	SHMT2
31	163	ISOC1
32	180	ZMYM3
33	83	H1FX
34	191	GOT2
35	262	AQR
36	214	KIF1BP
37	229	GTF2F2
38	246	PCID2
39	269	SCFD1
40	79	PLIN2
41	179	CDKN2A
42	198	CWF19L1
43	173	HMGB3
44	94	MATR3
45	37	EIF1AX
46	207	HMGB2
47	272	POLR2L
48	123	RFC5
49	24	AKAP8
50	110	GPKOW

Imp-5

Z-score Rank 3rd	Z-score Rank 2nd	Gene Name
1	1	IPO5
2	11	NFYA
3	17	DDX56
4	42	HK2
5	26	TP53I3
6	27	BOP1
7	6	THOC1
8	132	SPIN1
9	146	FBL
10	117	C5orf24
11	156	PDS5B
12	189	RBM39
13	52	LSM14A
14	165	ENOPH1
15	44	DIDO1
16	236	CDC42BPB
17	195	XRN2
18	175	U2AF1
19	131	MAP7D1
20	150	SNX5
21	278	DEK
22	142	RAVER1
23	94	MFAP1
24	76	TUFM
25	22	NADKD1
26	145	CPSF7
27	51	PTPN1
28	308	GBE1
29	119	GNB2
30	368	CD44
31	184	PHF6
32	153	MBD2
33	188	DDX46
34	226	ZNF146
35	12	SNX12
36	420	GAR1
37	418	LUC7L
38	182	SNRNP27
39	218	U2AF2
40	326	MAZ
41	114	PLOD3
42	380	SRSF7
43	367	HSPA9
44	370	ISOC1
45	379	SRSF3
46	449	RAB31
47	510	SDHA
48	369	SRSF8
49	344	PLRG1
50	451	NUCKS1
51	514	DDX17
52	479	LUC7L2
53	137	HNRNPA0
54	155	ACTR10
55	306	RPL22
56	357	ARL6IP4
57	271	UBE4B
58	275	PLIN2
59	477	HNRNPL
60	527	PRC1
61	500	SIN3B
62	375	RBM26
63	466	ADAR

Imp-7

Z-score Rank 3rd	Z-score Rank 2nd	Gene Name
1	2	TRAP1
2	9	ZNF787
3	25	ERP44
4	23	HMGB2
5	37	HIST1H4A
6	47	HNRNPUL1
7	29	ZNF207
8	51	ACADVL
9	63	BUB3
10	16	VIM
11	40	NUP155
12	80	DIDO1
13	53	HMGB3
14	44	FKBP10
15	65	ZNF146
16	72	GOT2
17	83	ZNF24
18	70	SDHA
19	39	SHMT2
20	102	H1FX
21	105	SRSF1
22	68	SRSF2
23	115	LUC7L3
24	89	OXCT1
25	86	SRSF7
26	173	PRPF6
27	67	FXR1
28	148	RSRC2
29	132	MAZ
30	217	SF3B5
31	50	TUFM
32	166	CDC5L
33	146	ACIN1
34	81	SRSF11
35	207	SNRPA1
36	208	ARL6IP4
37	183	SNRPB2
38	219	CDK12
39	26	HSPD1
40	206	SF3A1
41	97	SLC27A2
42	155	HMGB1
43	204	ARGLU1
44	253	RAB31
45	295	RPN1
46	151	GNB1
47	140	IFI16
48	117	SNRPA
49	165	HNRNPA3
50	177	SF3A2
51	282	SF3B2
52	22	NNT
53	260	SNRPD3
54	240	RAP1B
55	311	SF3B4
56	286	THBS1
57	222	SF3A3
58	228	SNRPB

Imp-8

Z-score Rank 3rd	Z-score Rank 2nd	Gene Name
1	4	ZNF787
2	6	TFRC
3	10	HSPD1
4	12	NOP56
5	3	RALY
6	34	MAZ
7	40	RPL11
8	42	RPL22
9	28	GOT2
10	7	HIST1H4A
11	36	SLC25A1
12	60	ZNF24
13	25	NNT
14	88	ARMC1
15	89	RAB14
16	19	DDX21
17	67	RAB1A
18	77	RBM3
19	21	NFYA
20	99	RAB2A
21	43	SNX27
22	61	RAB8A
23	63	FKBP10
24	103	LGALS1
25	78	RAB21
26	10	SHMT2
27	106	GOLPH3
28	127	DDX3X
29	101	RAB1B
30	93	RAB10
31	125	HK1
32	146	THBS1
33	29	CCAR1
34	134	LUC7L3
35	148	U2AF1
36	20	VIM
37	165	NUDT21
38	149	ACIN1
39	120	SRSF7
40	177	HNRNPH3
41	191	ELAVL1
42	39	U2SURP
43	166	MYO1B
44	197	ACSL4
45	128	U2AF2
46	62	RAB13
47	118	SRSF3
48	217	SF3B4
49	196	MYO1C
50	193	G3BP1
51	172	DDX6
52	50	HNRNPUL1
53	147	SF3B1
54	136	RPL30
55	207	SF3B5
56	69	RAB31
57	153	EIF3L
58	91	FIS1
59	81	SRSF11
60	221	SUB1

Imp-9

Z-score Rank 3rd	Z-score Rank 2nd	Gene Name
1	3	H2AFZ
2	1	ACAT1
3	13	CYR61
4	16	RALY
5	4	FUBP1
6	5	RBMX
7	44	GOT2
8	49	IVD
9	45	TFRC
10	18	CS
11	7	PRPF6
12	31	HSPA9
13	9	HNRNPUL1
14	12	SUPT16H
15	84	BMS1
16	75	ZNF787
17	55	KMT2A
18	78	MAZ
19	47	SHMT2
20	25	DHX30
21	151	SRRM2
22	146	SART1
23	157	H1F0
24	62	PDHB
25	191	PRPF3
26	130	WDR74
27	211	RPL27A
28	30	JUP
29	131	ACAA2
30	23	DDX17
31	81	RPS2
32	194	PPP1R10
33	229	SF3B5
34	92	ALYREF
35	166	WBSCR22
36	43	MYOF
37	214	DDX24
38	149	YY1
39	165	RPL23A
40	193	RPL35A
41	208	NUP98
42	284	LMNB1
43	250	PPIB
44	170	CELF1
45	205	RPL15
46	274	SSRP1
47	54	BCLAF1
48	156	SNRPA1
49	73	CD55
50	262	RPL7A
51	88	BBX
52	128	RPL36
53	326	RPL27

Imp-11

Z-score Rank 3rd	Z-score Rank 2nd	Gene Name
1	9	RALY
2	12	TFRC
3	34	AKR1C1
4	24	EIF4A3
5	53	RBM25
6	11	ACO2
7	36	ALDH18A1
8	91	ACP1
9	43	ESYT2
10	47	RBM39
11	120	GLOD4
12	41	LRRFIP1
13	124	MACROD1
14	140	CKAP5
15	25	IL18
16	173	RDX
17	185	MSN
18	49	AFG3L2
19	127	LGALS1
20	116	TMA7
21	177	U2AF1
22	143	NEDD8
23	62	HIST1H4A
24	172	DTYMK
25	187	APRT
26	167	LANCL2
27	198	MRTO4
28	216	VPS45
29	221	NCOR2
30	110	TBL1XR1
31	186	ARHGDIA
32	255	RPL35A
33	162	CLINT1
34	121	ACYP1
35	98	RAD23A
36	215	TXNL1
37	101	GDI2
38	189	KTN1
39	26	MYL12A
40	286	U2AF2
41	3	JUP
42	52	LPP
43	70	CCBL2
44	73	DDX46
45	318	SERPINB6
46	200	TBCB
47	223	RPL34
48	328	BTF3
49	304	RPL18A
50	85	RTF1
51	153	GALK1
52	349	NPEPPS

Imp-13

Z-score Rank 3rd	Z-score Rank 2nd	Gene Name
1	1	NFYB
2	5	LRRC59
3	6	GTF2A2
4	8	MAGOH
5	9	RBM8A
6	19	CHRAC1
7	23	POLE3
8	12	DDX27
9	33	NFYA
10	10	NOC2L
11	60	NQO2
12	34	SRSF8
13	98	TMEM43
14	63	ARPC5
15	174	TXNDC17
16	143	SFPQ
17	99	CDC42BPB
18	86	NAPRT1
19	73	BOLA2
20	76	TIGAR
21	100	RBM27
22	111	COMT
23	130	RPL37
24	118	SUMO2
25	226	RAVER1
26	7	UGGT1
27	224	MAP7
28	24	CAPN1
29	234	SMARCE1
30	62	ENOPH1
31	250	ZYX
32	56	EEF2
33	132	PRC1
34	279	TIMM8A
35	292	WDR18
36	172	CBS
37	18	PHF10
38	195	NAT10
39	309	SUMO3
40	278	GNPDA1
41	157	DBI
42	228	BROX
43	377	EEFSEC
44	148	GOLGA4
45	379	CLTC
46	324	IKBKAP
47	384	G6PD
48	189	S100A13
49	412	AHNAK
50	316	ZNF787
51	406	GEMIN5
52	233	GRWD1
53	83	SRSF2
54	453	PPIE
55	357	SRSF3
56	47	PELP1
57	215	TXLNG
58	244	UBE2I
59	478	APEH
60	425	KRT8
61	475	LIN7C
62	229	UTP18
63	231	PPP1R12A
64	401	RPL11
65	162	MARCKSL1
66	397	KRT17

Exp-4

Z-score Rank 3rd	Z-score Rank 2nd	Gene Name
1	3	DDX39B
2	4	DDX39A
3	9	JUP
4	23	VIM
5	25	XRN2
6	8	TMPO
7	24	HSPD1
8	35	ALDH1B1
9	31	CS
10	67	TFRC
11	7	SLTM
12	34	TOMM70A
13	36	PSIP1
14	13	NOP56
15	75	ALYREF
16	82	HNRNPA0
17	120	GTF2I
18	89	FAM32A
19	98	ZNF638
20	103	CPSF6
21	78	RBMX
22	105	SUMF2
23	122	RRBP1
24	115	FBL
25	135	EXOSC1
26	42	SFPQ
27	134	THBS1
28	136	RBM26
29	156	NONO
30	155	LUC7L2
31	62	CPSF7
32	193	CDC73
33	70	ARL6IP4
34	66	U2AF1
35	93	RBM39
36	34	ERH
37	61	WDR33
38	99	GAR1
39	189	CD55
40	153	MAP7
41	170	SUMO1
42	39	HIST1H4A
43	177	HNRNPA1
44	171	PTBP1
45	233	RAP1B
46	147	RAB35
47	146	SCAF11
48	53	ARGLU1
49	92	SRSF3

Figure 3. 3rd-Z-4% cargoes of the 12 NTRs. The 3rd-Z-4% cargoes of each NTR are listed by the gene names in the 3rd-Z-rank orders. The ranks by the second Z-scores are also shown. The 3rd-Z-4% and 2nd-Z-15% cargoes are indicated by cyan in the rank columns. Colors in the gene name columns: magenta, reported cargoes; blue, cargoes bound directly to the NTR in the bead halo assays (***Supplementary file 2***); light blue, cargoes bond directly to Imp-α but not to Imp-*β*; gray, proteins that did not bind to the NTRs; and yellow, Imp-α. For the 2nd-Z-15% cargoes, see ***Supplementary file 3***.
DOI: 10.7554/eLife.21184.011

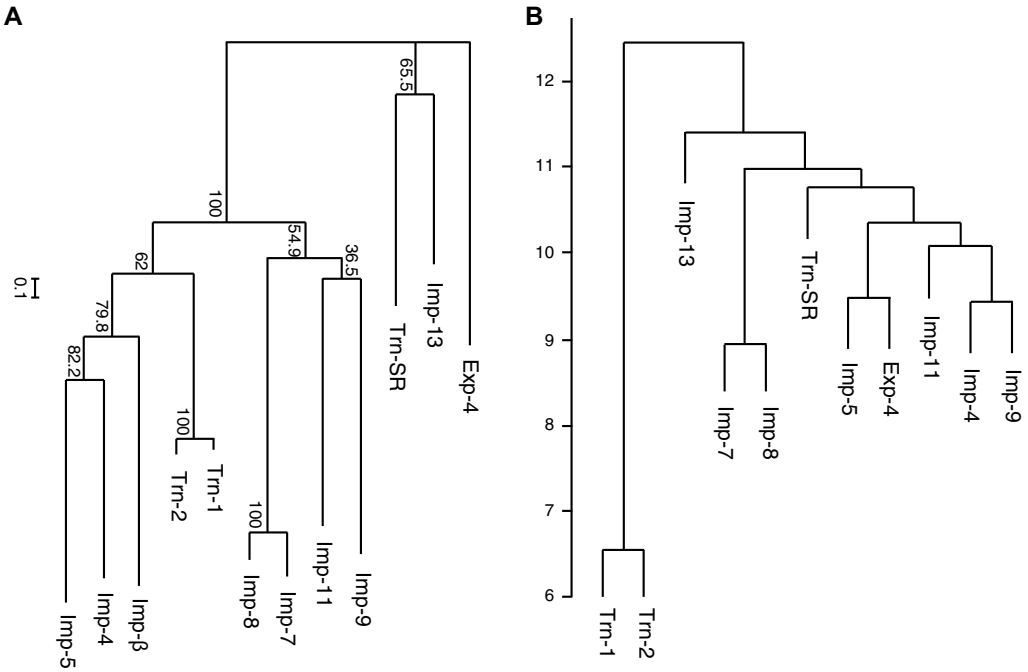

C

	Trn-1	Trn-2	Trn-SR	Imp-4	Imp-5	Imp-7	Imp-8	Imp-9	Imp-11	Imp-13	Exp-4	Unique	Total in 3rd-Z-4%
Imp-β	4	2	3	5	3	5	5	6	0	4	3	42	63
Trn-1		28	2	0	4	5	5	3	3	3	6	15	49
Trn-2			2	1	5	4	7	4	2	3	5	12	50
Trn-SR				4	10	4	6	2	1	4	4	36	63
Imp-4					4	7	4	7	1	1	4	25	49
Imp-5						8	8	3	4	7	11	23	62
Imp-7							19	8	1	2	7	22	58
Imp-8								8	6	4	8	24	60
Imp-9									4	1	6	28	53
Imp-11										0	5	39	52
Imp-13											3	46	66
Exp-4												20	49

Figure 4. Phylogenetic tree and cargo profile hierarchical clustering of the Imp-β family import receptors. (**A**) Phylogenetic tree of the 12 Imp-β family import receptors with the bootstrap values. Scale bar indicates substitutions per site. (**B**) A hierarchical clustering dendrogram of the same NTRs (except Imp-β) based on the similarities of their 3rd-Z-4% cargo profiles. Imp-β was excluded because Imp-α connects to Imp-β and many of the identified cargoes. The scale indicates the intercluster distance. (**C**) The numbers of 3rd-Z-4% cargoes shared by two NTRs. For the 2nd-Z-15% cargoes, see ***Supplementary file 5A***.

DOI: 10.7554/eLife.21184.012

(***Figure 5***; ***Supplementary file 9***), which are terms for biological processes (BPs). These cargoes are also annotated with chromatin, which is a term for cellular component (CC; ***Figure 6A***; ***Supplementary file 9***), and DNA binding, which is for molecular function (MF; ***Figure 6B***; ***Supplementary file 9***), all related to DNA recombination and DNA conformation change. For another example, the Trn-SR cargoes are significantly annotated with a range of terms for BPs that are related to cell division or nuclear division and terms for CCs that include condensed chromosome, kinetochore, spindle, and centrosome. Similarly, most of the examined NTRs are linked to terms for BPs via the 3rd-Z-4% cargoes (***Figure 5***) as follows: Imp-β, -4, -7, and Trn-SR are linked to chromatin or chromosome organization; Imp-β, -4, and -13 are linked to DNA repair; Imp-β is linked to mRNA capping; Trn-SR and Exp-4 are linked to mRNA polyadenylation; Trn-1 and -2 are linked to mRNA stabilization; Trn-2, -SR, Imp-5, -9, and Exp-4 are linked to ribosome biogenesis or rRNA processing; Trn-SR is linked to protein folding, modification, ubiquitination, and catabolic process; and Imp-4 and -7 are linked to apoptosis. The NTRs are also consistently linked to the terms for CCs and MFs (***Figure 6***) as follows: Trn-SR, Imp-5, -9, and Exp-4 are linked to Cajal body; Imp-β is linked to cap-binding complex; and Trn-SR is linked to pre-mRNA binding, snoRNA binding, and RNA helicase activity.

Term ID	Term Name	Imp-β		Trn-1		Trn-2		Trn-SR		Imp-4		Imp-5		Imp-7		Imp-8		Imp-9		Imp-11		Imp-13		Exp-4		Total
		p	#	*p*	#	*p*	#	*p*	#	*p*	#	*p*	#	*p*	#	*p*	#	*p*	#	*p*	#	*p*	#	*p*	#	No.
GO:0006259	DNA Metabolic Process	8E-06	11	0.199	6	1	2	0.146	7	0.002	8	1	4	0.632	6	1	2	0.34	6	1	2	2E-04	10	8E-06	10	978
GO:0006310	DNA Recombination	0.503	4	1	1			1	2	0.008	5	1	1	0.019	5	1	2	1	1	1	1	1	3	0.008	5	298
GO:0006323	DNA Packaging	1	3	1	1			1	2	0.039	4			0.003	5	1	2	1	1	1	1	1	1	1	1	200
GO:0071103	DNA Conformation Change	0.312	4	1	1			1	2	1E-04	6			4E-04	6	0.244	4	1	1	1	1	1	1	1	1	263
GO:0032392	DNA Geometric Change	1	2							4E-04	4			0.061	3	1	2									63
GO:0010216	Maintenance of DNA Methylation	0.031	2																							6
GO:0000737	DNA Catabolic Process, Endonucleolytic									0.002	3			0.436	2			1	1							23
GO:0006281	DNA Repair	0.002	7	1	3			1	2	0.007	6	1	1	1	4	1	1	1	3	1	2	0.043	6	0.111	5	519
GO:0006289	Nucleotide-Excision Repair	0.475	3							0.005	4			1	1					1	1	0.017	4	1	1	116
GO:0006284	Base-Excision Repair	0.043	3					1	1	1	2			1	1											52
GO:0006325	Chromatin Organization	6E-07	11	1	3	1	3	0.313	6	0.062	6	1	5	1	4	1	1	0.943	5	1	4	0.374	6	1	4	768
GO:0031497	Chromatin Assembly	1	3	1	1			1	1	0.017	4			0.035	4	1	1	1	1	1	1	1	1	1	1	162
GO:0016568	Chromatin Modification	2E-05	9	1	2	1	1	0.967	5	1	3	0.967	5	1	1	1	1	1	2	1	3	1	5	1	4	614
GO:0006338	Chromatin Remodeling	0.037	4	1	2					1	1	1	1	1	1	1	1			1	1	1	2	1	1	152
GO:0070828	Heterochromatin Organization	7E-04	3							1	1															14
GO:0051276	Chromosome Organization	4E-11	16	1	5	1	4	3E-06	12	2E-06	11	0.348	7	0.021	8	1	4	0.723	6	1	4	0.43	7	0.497	6	1126
GO:0032200	Telomere Organization	0.031	4	1	2	1	1	1	3	1	1	1	1	1	1	1	1			1	1	1	1	0.414	3	145
GO:0006368	Transcription Elongation from RNA Polymerase II Promoter	1E-04	5			1	1	1	2	0.118	3							1	2	1	1	1	2	1	1	95
GO:0016458	Gene Silencing	1E-05	7	1	2	1	2	1	2	1	1	1	2	1	2	1	2	1	3	1	1			1	1	244
GO:0034660	ncRNA Metabolic Process	3E-06	9	0.986	4	1	4	0.312	5	1	2	0.023	6	1	3	1	3	0.107	5	1	2	0.358	5	1	4	480
GO:0034470	ncRNA Processing	0.046	5	0.241	4	0.307	4	0.054	5	1	1	0.054	5	1	1	1	3	0.018	5	1	2	0.954	4	0.272	4	331
GO:0006370	7-Methylguanosine mRNA Capping	6E-12	7							0.616	2															33
GO:0000387	Spliceosomal snRNP Assembly	1	2			1	1							0.017	3			0.012	3			1	1			41
GO:0000389	mRNA 3'-Splice Site Recognition													3E-05	3											6
GO:0006378	mRNA Polyadenylation					1	1	0.018	3	1	1					1	1							0.007	3	37
GO:0098789	pre-mRNA Cleavage Required for Polyadenylation	0.031	2																							6
GO:0000184	Nuclear-Transcribed mRNA Catabolic Process, Nonsense-Mediated Decay	1	2	1	2	0.006	4					1	1			0.454	3	3E-10	8	0.008	4	0.021	4			123
GO:0048255	mRNA Stabilization	1	1	0.005	3	0.006	3			1	1	1	1			1	1							1	1	34
GO:0010501	RNA Secondary Structure Unwinding							0.032	3			0.032	3			0.023	3	1	2	1	2	1	1	1	2	45
GO:0042254	Ribosome Biogenesis	0.203	4	0.064	4	0.003	5	4E-04	6	1	2	0.236	4			0.158	4	5E-08	8	0.1	4	0.26	4	0.073	4	235
GO:0006364	rRNA Processing	1	2	0.456	3	0.557	3	0.001	5	1	1	0.047	4			0.894	3	0.019	4	1	2	0.052	4	0.014	4	155
GO:0042273	Ribosomal Large Subunit Biogenesis	1	1			1	2	1	2			1	1			1	1	0.014	3	1	1	1	1			43
GO:0006412	Translation	1	3	0.333	5	1E-04	8	1	5	1	2	1	4	0.895	5	2E-06	10	1E-05	9	1	4	0.001	8	1	3	677
GO:0006413	Translational Initiation	1	2	1	1	0.006	5	1	1	1	1	1	1			0.014	5	2E-07	8	1	3	1	2			273
GO:0006414	Translational Elongation					0.062	4					1	2	1	1	1	3	3E-08	8	0.076	4	0.198	4			219
GO:0006415	Translational Termination					0.028	4					1	1			1	3	6E-09	8	0.973	3	1	3			179
GO:0006457	Protein Folding			1	1			0.012	5	1	3	1	1	0.162	4	1	2	1	2	1	2	1	2	1	1	240
GO:0061077	Chaperone-Mediated Protein Folding							1	2	1	1			0.032	3	1	2	1	1					1	1	51
GO:0010608	Posttranscriptional Regulation of Gene Expression	8E-04	7	0.003	6	0.068	5	0.017	6	1	3	1	3	1	3	0.01	6	1	1	1	1	0.277	5	0.902	4	454
GO:0043412	Macromolecule Modification	0.024	15	1	7	1	5	2E-04	18	0.617	11	1	10	0.807	12	1	7	1	6	1	9	0.832	13	0.617	11	4139
GO:0036211	Protein Modification Process	1	11	1	6	1	4	0.004	16	0.42	11	1	9	0.538	12	1	6	1	6	1	9	0.542	13	1	9	3959
GO:0016567	Protein Ubiquitination	1	1			1	1	0.036	7	1	3	1	1	1	2					1	1	1	1	1	1	784
GO:0018205	Peptidyl-Lysine Modification	0.007	6	1	1	1	1	1	2	1	2			1	1			1	2	1	1	0.149	5	1	1	398
GO:0031145	Anaphase-Promoting Complex-Dependent Proteasomal Ubiquitin-Dependent Protein Catabolic Process							4E-04	5	1	2			1	2											120
GO:0030163	Protein Catabolic Process	1	1	1	3	1	1	0.005	8	1	4	1	2	1	2					1	5	1	3	1	1	827
GO:0007049	Cell Cycle	5E-05	13	1	4	1	3	0.004	11	0.15	8	1	6	1	7	1	7	1	2	1	4	1	6	0.15	8	1796
GO:0000278	Mitotic Cell Cycle	2E-04	10	1	3	1	1	0.025	8	0.033	7	1	3	1	5	1	5	1	1	1	3	1	4	1	2	1038
GO:0051301	Cell Division	1	4	1	1	1	1	0.001	8	1	4	1	2	1	2	1	1			1	1	1	2	1	1	672
GO:0000075	Cell Cycle Checkpoint							5E-04	6	1	3	1	1	1	3									1	1	249
GO:0071173	Spindle Assembly Checkpoint							4E-04	4	1	2			1	2											46
GO:0007091	Metaphase/Anaphase Transition of Mitotic Cell Cycle							1E-03	4	1	2			1	2											59
GO:0007059	Chromosome Segregation	1	3	1	1			0.024	5	0.141	4	1	1	1	2	1	1					1	2	1	1	279
GO:0000280	Nuclear Division	0.042	6	1	1			0.004	7	1	4	1	1	1	2					1	1	1	3			550
GO:0007077	Mitotic Nuclear Envelope Disassembly	0.026	3					1	2	1	1			1	1			1	1							44
GO:0048856	Anatomical Structure Development	1	12	0.057	14	0.102	14	0.503	15	1	10	1	11	0.009	17	3E-06	22	1	12	1E-05	20	0.231	16	0.329	13	5272
GO:0048731	System Development	1	11	0.224	12	1	11	1	13	1	8	1	10	0.107	14	0.035	15	1	10	0.034	14	1	13	1	10	4482
GO:0048869	Cellular Developmental Process	1	8	0.461	11	0.735	11	1	12	0.025	13	1	6	1	11	7E-05	18	1	7	0.002	15	1	11	0.127	12	4112
GO:0030154	Cell Differentiation	1	8	1	10	1	10	1	12	0.336	11	1	6	1	11	2E-04	17	1	7	0.001	15	1	10	0.069	12	3859
GO:0001649	Osteoblast Differentiation	1	3					1	2	1	2	1	2			1	1	1	2			1	1	0.046	4	209
GO:0003012	Muscle System Process	1	1	1	1	1	2	1	1					1	3	1	1	1	2	1	2	1	1	0.031	5	398
GO:0012501	Programmed Cell Death	1	8	1	3	1	1	0.326	9	0.034	9	1	8	0.003	11	0.179	9	0.384	8	1	3	1	5	1	7	1921
GO:0097194	Execution Phase of Apoptosis	1	1					1	1	0.122	3			0.004	4	1	2	1	2					1	1	96
GO:0030262	Apoptotic Nuclear Changes									0.004	3			0.006	3	1	1	1	1							30
GO:0006309	Apoptotic DNA Fragmentation									7E-04	3			0.264	2			1	1							18
GO:0009607	Response to Biotic Stimulus	1	5	1	4	1	3	1	5	1	2	1	3	0.008	8	0.089	7	1	2	1	1	1	3	1	4	984
GO:0006974	Cellular Response to DNA Damage Stimulus	0.037	7	1	4			1	5	3E-05	9	1	3	1	5	1	1	1	4	1	3	0.5	6	0.007	7	811
GO:0006979	Response to Oxidative Stress			1	3	1	2	1	2	1	1			1	3	1	2			1	1	1	4	0.033	5	401
GO:0070887	Cellular Response to Chemical Stimulus	1	9	0.103	10	0.842	9	1	10	1	6	1	9	0.124	11	0.16	11	0.007	12	2E-06	16	1	9	0.003	12	2852
GO:0014070	Response to Organic Cyclic Compound	1	2	1	4	1	3	1	4	1	3	1	2	0.382	6	1	5	1	3	1E-04	9	1	4	1	4	890
GO:1901698	Response to Nitrogen Compound	1	1	1	3	1	4	1	5			1	5	1	6	0.019	8	1	2	1	3	1	1	1	5	1087
GO:1901700	Response to Oxygen-Containing Compound	1	3	1	5	1	6	1	6	1	4	1	5	0.006	10	0.058	9	1	6	0.021	9	1	4	0.086	8	1660
GO:0010038	Response to Metal Ion	1	1	0.014	5	1	3	1	2	1	1			1	1	1	2	1	2	1	2	1	2	1	2	349
GO:0006952	Defense Response	1	4	1	2	1	3	1	3	1	7	1	5	0.018	10	0.144	9	1	3	1	3	1	3	1	6	1867
GO:0002376	Immune System Process	1	6	1	3	1	4	1	6	0.002	12	1	6	0.069	11	0.003	13	1	5	1	7	1	6	1	8	2673
GO:0032606	Type I Interferon Production	1	1					1	1	0.006	4			0.013	4	1	2			1	1			1	1	127
GO:0007165	Signal Transduction	1	11	1	10	1	10	0.009	19	1	9	0.479	16	0.036	17	1E-04	21	1	9	0.009	17	1	13	0.244	14	5865
GO:0007154	Cell Communication	1	12	1	12	1	10	0.008	20	1	11	0.119	18	0.03	18	2E-05	23	1	10	0.001	19	0.215	18	0.165	15	6420
	No. in Top 4%		63		49		50		63		49		62		58		60		53		52		66		49	

Figure 5. GO term (Biological Process) enrichments of the 3rd-Z-4% cargoes. The 3rd-Z-4% cargoes were analyzed for GO term (term type, Biological Process) enrichment. The significantly enriched terms (p<0.05, cyan) in the 3rd-Z-4% cargoes of four or fewer NTRs were selected, and a representative term for each group of highly similar is presented with their p-values and the numbers (#) of cargoes annotated with them. Total No. denotes the number of proteins annotated with each term in the database. Related terms are bundled in the same color. This table was extracted from

Figure 5 continued on next page

Figure 5 continued

Supplementary file 6B. All the GO terms annotated to the 3rd-Z-4% cargoes are listed in ***Supplementary file 7***. The correspondence between each 3rd-Z-4% cargo and GO term is summarized in ***Supplementary file 9***. For the 2nd-Z-15% cargoes, see ***Supplementary files 6A***, ***8,*** and ***10***.
DOI: 10.7554/eLife.21184.013

Nearly twice as many GO terms were annotated to the 2nd-Z-15% cargoes. The correspondences between the 2nd-Z-15% cargoes of the 12 NTRs and selected representative GO terms enriched significantly for them are tabulated in ***Supplementary file 10***. The excerpted list of terms enriched significantly for the cargoes of four or fewer NTRs contains terms partially different from those in ***Figures 5*** and ***6*** (***Supplementary file 6A***), but many of the NTRs are still linked to terms similar to those of the 3rd-Z-4% cargoes. For example, Imp-β and Trn-SR are linked to terms related to cell or nuclear division by the 3rd-Z-4% cargoes (***Figure 5***) and to partially different terms that are still related to cell or nuclear division by the 2nd-Z-15% cargoes (***Supplementary file 6A***). Additionally, Imp-4 is linked to terms related to DNA structure regulation, DNA repair, and apoptosis in both lists. Similarly, most of the examined NTRs are linked in both lists to similar terms that are related to any of the following: chromatin organization, chromosome organization, DNA repair, ribosome biogenesis, protein modification, cell division, nuclear division, and apoptosis. Thus, we regard the 3rd-Z-4% list as a core table of the cargo roles. Naturally, the 2nd-Z-15% cargoes linked the NTRs to additional terms (***Supplementary file 6A***) as follows: Imp-β, -4, and Trn-SR are linked to DNA-dependent DNA replication; Trn-1 and Imp-7 are linked to gene silencing by RNA; Imp-β, -7, and -13 are linked to rRNA transcription; Imp-β and Trn-SR are linked to protein methylation; Trn-SR is linked to protein peptidyl-prolyl isomerization; Trn-2, Imp-4, and -8 are linked to circadian rhythm; Imp-β, -4, -13, and Trn-SR are linked to terms for CCs and MFs that are related to RNA polymerase (RNAP) II transcription; and subsets of the NTRs are linked to varying terms that are related to differentiation, development, and response. As an important result, we have illustrated the general framework of the division of roles among the NTRs for the first time, in which one NTR is linked to many BPs and conversely each broadly defined BP is supported by many NTRs, but each closely defined BP is supported by a restricted number of NTRs. One typical example is the allocation of mRNA processing factors (see below).

Allocation of mRNA processing factors to the NTRs

Some of the GO terms related to mRNA processing were specifically linked to four or fewer NTRs by the 3rd-Z-4% and 2nd-Z-15% cargoes (***Figure 5***; ***Supplementary file 6A***). However, many other terms related to mRNA processing were linked to more NTRs, and conversely, all the NTRs were implicated in mRNA processing. The 2nd- and 3rd-Z-rankings for the 12 NTRs included 275 and 242 proteins, respectively, that were annotated with mRNA processing (***Supplementary file 6B and 6C***). To see the allocation of these proteins to the NTRs, the ranks of these proteins are arranged in a table (***Supplementary file 11A***). The 2nd- and 3rd-Z-rankings revealed similar results. As summarized for the 2nd-Z-ranking (***Figure 7***), particular groups of the mRNA-processing factors are allocated to specific NTRs, showing that each NTR is linked to distinct reactions in mRNA processing: the proteins related to mRNA capping are allocated to Imp-β almost exclusively; hnRNP A0 is allocated to Trn-1, -2, Imp-4, -11, and others; hnRNP A1, A2B1, A3, D, F, H1–3, and M are allocated to Trn-1 and -2, and additionally Imp-9 and Exp-4; hnRNP U-like 1 are allocated to Imp-7, -8, and -9; SR-rich SFs are primarily allocated to Trn-SR and secondarily to Imp-7, -8, and -9; SFs 3A and B are allocated to Imp-4, -7, -8, -9, -11, and Exp-4; PQ-rich SF is allocated to Imp-4, -7, -8, and Exp-4; snRNP A–C is allocated to Imp-4, -7, -8, and Exp-4; exon junction complex (EJC) components are exclusively allocated to Imp-11 and -13; cleavage and polyadenylation specificity factor (CPSF) 1 is allocated to Imp-7 and -9; CPSF5 (NUDT21), 6, and 7 are less specifically allocated to other NTRs; general transcription factor IIF is allocated to Imp-β, -4, and Trn-SR; and RNAP II associating factors are allocated to Trn-SR and separately to other NTRs. Thus, the NTRs import distinctive subsets of mRNA processing factors. In the 2nd-Z-ranking, the SR-rich SFs were not allocated to Imp-5, but they were identified as the Imp-5 3rd-Z-4% cargoes. Thus, subsets of proteins involved in a broadly defined BP, for example, mRNA processing, are allocated to different NTRs, in a manner representative of role division among the NTRs.

A

Term ID	Term Name	Imp-β		Trn-1		Trn-2		Trn-SR		Imp-4		Imp-5		Imp-7		Imp-8		Imp-9		Imp-11		Imp-13		Exp-4		Total
		p	#	*p*	#	*p*	#	*p*	#	*p*	#	*p*	#	*p*	#	*p*	#	*p*	#	*p*	#	*p*	#	*p*	#	No.
GO:0008622	Epsilon DNA Polymerase Complex																					0.024	2			5
GO:0044452	Nucleolar Part	1	2	1	1	0.033	3	0.076	3	1	1	0.076	3			1	2					1	1	3E-04	4	60
GO:0015030	Cajal Body	1	1					6E-04	4			6E-04	4			1	1	0.024	3	1	2			0.019	3	52
GO:0042382	Paraspeckles			1	1	1	1			1	1					1	1					1	1	2E-05	3	6
GO:0034399	Nuclear Periphery	1	1	1	2	1	1	1	1	0.249	3	1	1			1	1	0.31	3	1	1	1	2	0.006	4	122
GO:0005635	Nuclear Envelope	2E-05	8	1	1	1	1	1	1	1	2	1	1	1	1	1	1	1	3	1	1	0.172	5	1	2	410
GO:0000785	Chromatin	0.012	6	0.724	4	1	1	1	2	1E-04	7	1	3	1	3	1	2	0.073	5	1	2	1	3	0.003	6	442
GO:0000791	Euchromatin									1	1							0.005	3					1	1	31
GO:0098687	Chromosomal Region	1	3	1	2			2E-06	8	1	1	1	3	1	3	1	1			1	1	1	3	1	3	301
GO:0000793	Condensed Chromosome	1	3	1	1			0.004	5	0.032	4	1	1	0.067	4							1	1			191
GO:0000776	Kinetochore							0.015	4	1	1	1	1	1	2							1	2			116
GO:0005819	Spindle	1	3	1	1			4E-05	7	1	1	0.455	4	1	2					1	2	1	2			279
GO:0005813	Centrosome			1	1	1	1	0.001	7	1	2					1	2			1	1	1	2			476
GO:0090575	RNA Polymerase II Transcription Factor Complex	0.006	4	1	2	1	2			1	2	1	1			1	1					0.008	4	1	2	96
GO:0016602	CCAAT-Binding Factor Complex											1	1			1	1					0.014	2			4
GO:0005845	mRNA Cap Binding Complex	1E-06	4																							12
GO:0005732	Small Nucleolar Ribonucleoprotein Complex	1	1	1	1	1	1	1	1			0.441	2			1	1							0.001	3	20
GO:0030532	Small Nuclear Ribonucleoprotein Complex					1	1					1	2	1E-19	11	0.054	3	4E-06	5					1	1	60
GO:0097525	Spliceosomal snRNP Complex					1	1					1	2	3E-20	11	0.037	3	2E-06	5					1	1	53
GO:0005684	U2-Type Spliceosomal Complex											0.008	3	5E-10	6	0.006	3			1	1			1	1	29
GO:0089701	U2AF							1	1			0.002	2			0.002	2			0.001	2			1	1	2
GO:0005849	mRNA Cleavage Factor Complex							1	1			1	1			1	1							3E-04	3	14
GO:0044391	Ribosomal Subunit					0.019	4			1	1	1	1			1	3	3E-09	8	0.727	3	1	2			162
GO:0031428	Box C/D snoRNP Complex			1	1	1	1					1	1			1	1							0.018	2	6
GO:0005856	Cytoskeleton	0.293	9	1	5	1	3	2E-04	13	1	5	1	7	1	4	1	6	1	5	0.001	11	0.014	11	1	4	1949
GO:0010494	Cytoplasmic Stress Granule	1	1	1	1	1	1	1	2			1	1			0.008	3									32
GO:0044445	Cytosolic Part					0.048	4			1	2	1	1			1	3	2E-08	8	1	3	1	2			205
GO:0005739	Mitochondrion	0.622	8	1	5	1	4	1	4	0.102	8	1	5	9E-04	11	1E-05	13	3E-04	11	0.003	10	0.966	8	0.102	8	1699
GO:0005783	Endoplasmic Reticulum	1	2	1	3	1	4	1	1	1	5	1	3	1	6	8E-04	11	1	1	1	2	1	4	1	5	1623
GO:0005768	Endosome	1	1	1	1	1	2	1	4	1	3	1	4	1	3	2E-08	12	1	1	1	2	1	1	1	3	779
GO:0005794	Golgi Apparatus			1	2	1	2	1	3	1	5	1	2	1	2	2E-04	11	1	3	1	3	1	5	1	2	1436
GO:0031410	Cytoplasmic Vesicle	1	1	1	2	1	2	1	4	1	5	1	3	1	4	3E-07	13	1	4	1	2	1	1	1	5	1232
GO:0005925	Focal Adhesion	1	2	1	1	1	2			1	1	1	4	1	1	0.004	6	0.002	6	0.039	5	0.008	6	1	2	383
GO:0005905	Coated Pit			1	1					1	2			1	1	1	2	1	1	1	1	1	1	0.033	3	62
GO:0043209	Myelin Sheath	1	1							1	2	1	3	0.047	4	1	2	1	2	0.032	4	1	1	1	1	175
	No. in Top 4%	63		49		50		63		49		62		58		60		53		52		66		49		

B

Term ID	Term Name	Imp-β		Trn-1		Trn-2		Trn-SR		Imp-4		Imp-5		Imp-7		Imp-8		Imp-9		Imp-11		Imp-13		Exp-4		Total
		p	#	*p*	#	*p*	#	*p*	#	*p*	#	*p*	#	*p*	#	*p*	#	*p*	#	*p*	#	*p*	#	*p*	#	No.
GO:0034061	DNA Polymerase Activity	0.008	3					1	1													1	2			30
GO:0003690	Double-Stranded DNA Binding	0.023	7	1	4	1	4	1	2	0.62	5	1	5	0.153	6	1	3	1	4			1	2	0.62	5	752
GO:0003697	Single-Stranded DNA Binding	1	1	0.001	4	1	2	1	1	1	2			0.164	3	1	2	1	1	1	2			1	2	88
GO:0098847	Sequence-Specific Single Stranded DNA Binding			0.039	2	0.046	2																	1	1	9
GO:0008301	DNA Binding, Bending									0.001	3			0.002	3											20
GO:0043566	Structure-Specific DNA Binding	0.289	3	1	1			1	1	0.002	4			0.226	3			0.162	3					1	1	98
GO:0000217	DNA Secondary Structure Binding									7E-04	3			0.001	3			1	1							18
GO:0000400	Four-Way Junction DNA Binding									5E-05	3			9E-05	3			1	1							8
GO:0097100	Supercoiled DNA Binding									0.007	2			0.011	2									1	1	4
GO:0003682	Chromatin Binding	8E-11	12	1	3	1	2	1	4	0.061	5	1	2	1	2	1	3	1E-05	8	1	1	1	4	0.924	4	457
GO:0042162	Telomeric DNA Binding			0.003	3	0.004	3																	1	1	30
GO:0001047	Core Promoter Binding	1	3	1	1	1	2	1	2	1	2	1	2	1	2	0.91	3	0.019	4			1	2	0.514	3	156
GO:0000988	Transcription Factor Activity, Protein Binding	3E-04	8	0.012	6	0.227	5	0.006	7	1	1	1	2	1	2	1	2	1	4	1	3	1	4	1	2	587
GO:0003727	Single-Stranded RNA Binding	1	2	2E-08	6	4E-04	4	1	1	1	1	1	2	1	1	1	2			1	2			1	2	62
GO:0036002	Pre-mRNA Binding			1	1	1	1	0.004	3			1	1	1	1	1	1			1	1	1	1	1	1	23
GO:0071208	Histone Pre-mRNA DCP Binding													0.011	2											4
GO:0003730	mRNA 3'-UTR Binding	1	1	0.015	3	0.018	3							1	1	1	1									49
GO:0017091	AU-rich Element Binding			0.001	3	0.002	3					1	1			0.432	2							1	1	23
GO:0017069	snRNA Binding	1	1	1	1	1	1	1	1					3E-07	5	1	1	1	1			1	1	1	1	34
GO:0035614	snRNA Stem-Loop Binding													0.002	2											2
GO:0004004	ATP-Dependent RNA Helicase Activity							2E-07	6	1	1	0.102	3			0.001	4	0.05	3	1	2	1	1	1	2	66
GO:0030515	snoRNA Binding	1	1	1	1	1	1	0.005	3			1	1			0.471	2							0.323	2	24
GO:0051082	Unfolded Protein Binding			1	1			0.009	4	1	1	1	1	1	2	1	1	1	2	1	1	1	1	1	1	102
GO:0019789	SUMO Transferase Activity																					4E-04	3			11
GO:0019901	Protein Kinase Binding	1	1	1	2	1	3	0.046	6	1	2	1	3	1	2	1	3	1	1	1	3	1	4	1	3	543
GO:0003988	Acetyl-CoA C-Acyltransferase Activity																	0.021	2							6
GO:0016887	ATPase Activity	1	4	1	1	1	1	0.008	6	1	1	1	3	1	2	1E-05	8	1	3	1	3	1	1	1	3	402
GO:0003924	GTPase Activity					1	3	1	1	1	1	1	3	0.126	4	2E-09	9					1	2	1	2	225
	No. in Top 4%	63		49		50		63		49		62		58		60		53		52		66		49		

Figure 6. GO term (Cellular Component and Molecular Function) enrichments of the 3rd-Z-4% cargoes. The 3rd-Z-4% cargoes were analyzed, and the results are presented in a format similar to that of ***Figure 5***. (**A**) Term type, Cellular Component. (**B**) Term type, Molecular Function. These tables were extracted from ***Supplementary file 6B***. All the GO terms annotated to the 3rd-Z-4% cargoes are listed in ***Supplementary file 7***. The correspondence between each 3rd-Z-4% cargo and GO term is summarized in ***Supplementary file 9***. For the 2nd-Z-15% cargoes, see ***Supplementary file 6A***, ***8,*** and ***10***.

DOI: 10.7554/eLife.21184.014

Accession	Major Feature	Gene Name	Rank by 2nd Z-score											
			Imp-β	Trn-1	Trn-2	Trn-SR	Imp-4	Imp-5	Imp-7	Imp-8	Imp-9	Imp-11	Imp-13	Exp-4
O43148	mRNA Capping	RNMT	2	1432	1420	1906	358	327	1487	1066	687	1560	598	447
Q09161	Cap-Binding	NCBP1	25	327	1037	1373	751	1466	906	1220	655	1248	594	1075
P52298		NCBP2	19			1416		1529	865			1510	602	
Q13151	hnRNP	HNRNPA0	247	11	13	145	50	137	92	422	105	7	558	82
P09651		HNRNPA1	245	7	7	285	364	776	323	438	171	773	641	177
P22626		HNRNPA2B1	301	16	19	382	555	902	336	420	160	711	531	123
P51991		HNRNPA3	634	13	14	531	260	823	165	163	182	405	987	210
P07910		HNRNPC	496	857	259	386	324	1140	337	570	117	563	676	229
Q14103		HNRNPD	851	8	8	566	623	1300	565	938	709	1237	1512	633
P52597		HNRNPF	1678	95	52	1702	382	211	268	230	608	1289	1251	304
P31943		HNRNPH1	438	34	40	948	171	723	233	325	243	628	646	202
P55795		HNRNPH2	741	41	42	1452	1126	534	363	280	302	802	573	208
P31942		HNRNPH3	373	167	85	753	708	686	221	177	177	394	404	184
P61978		HNRNPK	509	1130	331	351	611	919	459	569	318	982	580	315
P14866		HNRNPL	453	491	125	634	154	477	532	621	148	999	921	236
Q8WVV9		HNRPLL	145	1397	1430	1331	1281	774	320	542	479	1018	1056	212
P52272		HNRNPM	403	4	5	294	532	754	618	723	216	333	777	292
O60506		SYNCRIP	770	866	483	1123	503	508	435	529	575	808	628	693
O43390		HNRNPR	471	1421	133	374	1269	598	463	719	293	1236	674	388
Q00839		HNRNPU	123	837	205	395	415	1025	759	1247	475	1133	645	556
Q9BUJ2		HNRNPUL1	572	1600	1586	1503	354	1382	47	50	9	1253	1323	100
Q8IYB3	SR-Rich Splicing Factor	SRRM1		1440	1040	1977	863	1842			276	6		723
Q9UQ35		SRRM2	202	203	147	3	1412	1463	249	54	151	803	1872	355
Q07955		SRSF1	1617	328	113	55	984	1159	105	84	238	490	786	145
Q01130		SRSF2	133	234	143	8	156	628	68	85	152	373	83	164
P84103		SRSF3	274	294	254	90	243	379	110	118	49	236	357	92
Q13243		SRSF5	1002	213	378	524	538	833	457	659	212	1504	644	379
Q13247		SRSF6	1964	212	279	16	740	537	288	446	124	1091	1728	287
Q16629		SRSF7	377	553	592	26	200	380	86	120	85	224	232	79
Q9BRL6		SRSF8	115	738	1244	19		369					34	
Q05519		SRSF11	1194	342	162	1764	221	1199	81	81	93	338	1576	185
Q15459	Splicing Factor 3A, B	SF3A1	1621	442	366	1667	118	982	206	228	190	184	1313	150
Q15428		SF3A2	1623	402	320	1644	126	782	177	209	202	106	1414	133
Q12874		SF3A3	1650	375	291	1674	114	1021	222	243	231	227	1367	160
O75533		SF3B1	1660	343	273	1542	81	862	211	147	188	56	1326	84
Q13435		SF3B2	1638	432	276	1522	143	1000	282	206	178	214	1491	151
Q15393		SF3B3	1604	322	288	1516	172	999	316	352	192	71	1191	207
Q15427		SF3B4	1552	458	214	1566	215	1029	311	217	180	126	843	217
Q9BWJ5		SF3B5	1634	418	247	1478	265	1077	217	207	229	77	1317	188
Q9Y3B4		SF3B14	1663	336	246	1685	43	912	181	188	330	148	1483	131
Q01081	Splicing Factor U2AF	U2AF1	190	154	201	202	329	175	99	148	48	177	1476	66
P26368		U2AF2	261	360	342	1293	220	218	111	128	76	286	1107	106
P23246	PQ-Rich SF	SFPQ	111	219	1209	1890	31	1831	74	24	547	1542	143	42
P09012	snRNP A-F	SNRPA	1030	444	400	218	459	1063	117	142	218	415	1887	361
P09661		SNRPA1	1463	338	316	1664	112	976	207	231	156	107	1475	141
P14678		SNRPB	764	333	222	1540	238	795	228	143	210	226	736	219
P08579		SNRPB2	1422	311	257	1603	84	1050	183	216	144	268	1510	85
P09234		SNRPC	354	555	393	915	411	825	130	170	272	310	710	91
P62314		SNRPD1	743	300	241	1271	166	896	359	441	196	481	1602	364
P62316		SNRPD2	1199	604	238	1646	284	1308	352	493	311	342	1084	227
P62318		SNRPD3	843	384	226	1523	549	861	260	162	217	282	631	256
P62304		SNRPE	1512	357	203	1399	230	948	285	293	241	396	1458	431
P62306		SNRPF	584	426	466	893	73	1191	171	266	223	240	562	329
Q9Y5S9	Exon Junction Complex	RBM8A	497	517	505	976	783	1857	1614	1052	281	109	9	570
P38919		EIF4A3	629	289	392	256	394	998	535	852	490	24	737	681
P61326		MAGOH	1643	388	329	1183	484	1414	929	975	402	841	8	450
Q10570	Cleavage and Polyadenylation Specificity Factor	CPSF1	1029	690	1105	1481	231	1950	48	1236	56	1586	1837	114
Q9P2I0		CPSF2	825	578	351	309	1434	1326	917	1541	530	99	1856	1730
Q9UKF6		CPSF3	1104	1348	274	1367	1270	1666	1358	1664	663		1639	1359
O43809		NUDT21	415	335	99	157	593	253	254	165	154	590	1478	254
Q16630		CPSF6	281	647	368	125	201	289	125	96	121	738	687	103
Q8N684		CPSF7	187	521	191	62	421	145	158	208	89	138	1136	62
P35269	General Transcription	GTF2F1	35	587	192	68	64	685	224	846	416	466	210	309
P13984		GTF2F2	61	636	249	134	229	964	741	811	236	837	510	472
Q8N7H5	RNA Pol II Associating Factor	PAF1	1901	886	1304	14	579	1478	1224	827			1657	33
Q6P1J9		CDC73	1478	266	542	206	992	1355	484	1227	329	1635	1829	193
Q6PD62		CTR9	106	1398	91	189		29	159	79		760	1509	324
Q8WVC0		LEO1	1248	1271	792	272	624	1570	574	1601	187	1546	1277	404
P18615		NELFE	911	1482	1117	123	55	737	757	1317	487	1199	1891	882

Color Scale: Top 4% 4–8% 8–15%

Figure 7. mRNA processing factors in the 2nd-Z-rankings. The ranks of the mRNA processing factors in the 2nd-Z-rankings of the 12 NTRs are presented. The color scale is set by percentile rank as indicated. The 2nd-Z-rankings of the 12 NTRs include 275 proteins in total that are annotated with mRNA processing in GO. Of these, 69 were selected and are presented. For other factors and the 3rd-Z-rankings, see ***Supplementary file 11A***.
DOI: 10.7554/eLife.21184.015

Allocation of RPs to the NTRs

RPs migrate into the nuclei for ribosome assembly, but the NTRs responsible for import have been determined for only a few of RPs (***Chook and Süel, 2011***). The 3rd-Z-4% cargoes include 15 RPs (***Supplementary files 1***, ***5C,*** and ***11B***). To see the allocations of all the RPs to the NTRs, the ranks of

the RPs in the 2nd-Z-rankings are arranged in a table (***Figure 8***). Because the +NTR/Ctl values were obtained for most of the RPs in the three SILAC-Tp replicates, the second Z-scores are the median Z-scores in most cases, and they should fairly reflect the import efficiencies. Half of the RPs are included in the 2nd-Z-15% cargoes of one to five NTRs, and most of the RPs are ranked in the top 30% in the 2nd-Z-rankings of additional NTRs. Surprisingly, most RPs, especially the 60S subunit proteins, are ranked in the top 50% of most of the 2nd-Z-rankings, and few RPs are ranked lower. These findings imply that most of the RPs are allocated to multiple NTRs, but the import efficiencies vary depending on the NTR. Indeed, several RPs are reported cargoes of multiple NTRs (***Jäkel and Görlich, 1998***; ***Jäkel et al., 2002***). Imp-7, -8, and -9 primarily import RPs, Imp-11 and Exp-4 secondarily import RPs, and all other NTRs also contribute to the import of RPs to some extent. Among the highly homologous NTR pairs, Trn-2 and Imp-8 import RPs more efficiently than Trn-1 and Imp-7, respectively, which indicates that RP import is one of the roles shared unequally by similar NTRs. This differentiation is clearer in the 3rd-Z-rankings (***Supplementary file 11B***).

Allocation of transcription factors to the NTRs

Sequence-specific DNA-binding transcription factors (annotated with 'transcription factor activity, sequence specific DNA binding' in GO) play pivotal roles in many cellular processes, but they are not significantly enriched in the 3rd-Z-4% cargoes of any NTR (***Supplementary file 6B***). Transcription cofactors (annotated with 'transcription factor activity, protein binding'), which may engage in gene-specific transcription, are significantly enriched in the 3rd-Z-4% cargoes of only three NTRs (***Figure 6B***; ***Supplementary file 6B***). Nonetheless, transcription factors (sequence-specific DNA binding) are enriched in the Imp-β 2nd-Z-15% cargoes, and cofactors (protein binding) are enriched in the 2nd-Z-15% cargoes of 10 NTRs (***Supplementary file 6C***). Additionally, some transcription factors and cofactors are included in the 2nd-Z-15% cargoes, albeit not enriched. Thus, the 2nd-Z-15% cargoes of each NTR include 17 to 36 transcription factors or cofactors as listed at the bottom of ***Supplementary file 11D***. We performed GO analyses (term type, BP) for these transcription factors and cofactors (***Supplementary file 11C and 11D***). The annotated terms may reflect both direct transcription regulation activities and indirect effects via transcription. The proteins annotated with histone modification are enriched in the Imp-β and -13 cargoes, and the term may reflect their direct functions. The cargoes of several NTRs annotated with varying types of nuclear receptor signaling may act as cofactors in receptor-regulated transcription. In contrast, many of the transcription factors and cofactors identified as cargoes are annotated differently with various terms related to cell proliferation, development, rhythmic processes, or apoptosis and may act on these processes via transcriptional regulation. Thus, the NTRs import transcription factors and cofactors that work in distinct cellular processes.

Characterizations of the cargoes of individual NTRs

The GO analyses elucidated the characteristics of the NTR-specific cargoes, but the terms are annotated to not only the central players but also many indirect participants in BPs. Here, we primarily discuss the roles of the notable 3rd-Z-4% cargoes of each NTR and supplement this information with references to the 2nd-Z-15% cargoes. To make our points clear, we classified the 3rd-Z-4% and 2nd-Z-15% cargoes by their characteristics and their allocations to each NTR are presented in ***Supplementary file 5C and 5E***. We describe the features of the Imp-13 and Trn-SR cargoes first, because it includes the discussion on an export cargo or SR-domains. Biological functions linked to NTRs by the natures of their cargoes need to be verified by further experiments.

Imp-13 cargoes

Several Imp-13 cargoes have previously been reported, and our SILAC-Tp clearly reproduced the reported import specificities. Nuclear transcription factor Y subunits β (NFYB) and γ (NFYC) have been reported to be Imp-13 specific cargoes, whereas subunit α (NFYA), which has a BIB-like sequence, has been reported to bind to multiple NTRs (***Kahle et al., 2005***). NFYB is ranked first in both the Imp-13 2nd- and 3rd-Z-rankings, and NFYC is a 2nd-Z-15% cargo (***Figure 3***; ***Supplementary files 1*** and ***3***). Additionally, we identified NFYA as a cargo of multiple NTRs. Interestingly, a subunit of the general transcription factor TFIIA (GTF2A2) that interacts with NFYA (***Rolland et al., 2014***) is also a highly ranked Imp-13 3rd-Z-4% cargo. We could not identify the Imp-

			Rank by 2nd Z-score											
	Accession	Gene Name	Imp-β	Trn-1	Trn-2	Trn-SR	Imp-4	Imp-5	Imp-7	Imp-8	Imp-9	Imp-11	Imp-13	Exp-4
40S Subunit	P08865	RPSA	1112	1181	580	1143	442	599	568	436	520	514	805	640
	P15880	RPS2	1279	860	840	992	1095	859	633	488	481	565	740	594
	P23396	RPS3	1266	1058	645	1042	962	657	537	418	512	372	973	494
	P61247	RPS3A	1127	1047	859	1096	672	745	548	413	351	455	827	475
	P62701	RPS4X	1197	911	835	982	925	624	474	394	422	558	800	564
	P46782	RPS5	1094	967	678	1095	725	769	478	252	338	502	798	458
	P62753	RPS6	673	902	456	1173	590	829	507	502	395	522	791	369
	P62081	RPS7	1103	1031	907	1127	889	655	511	431	81	588	747	560
	P62241	RPS8	1161	1083	871	1020	927	691	530	464	424	503	691	489
	P46781	RPS9	1147	1016	699	963	704	626	392	404	366	523	880	535
	P46783	RPS10	924	1105	521	669	675	703	420	335	328	253	662	490
	P62280	RPS11	1170	1086	743	735	842	555	490	390	369	587	751	448
	P25398	RPS12	1110	1166	727	1033	1029	752	418	326	411	623	619	482
	P62277	RPS13	1087	830	888	1140	812	693	516	429	420	521	916	456
	P62263	RPS14	1089	1203	936	1248	1075	881	319	382	418	657	689	623
	P62841	RPS15	1373	908	691	997	1002	487	510	449	583	953	936	612
	P62244	RPS15A	1037	1263	862	1014	878	651	503	432	436	329	1020	546
	P62249	RPS16	1045	1041	763	966	957	588	517	369	371	583	821	653
	P0CW22	RPS17L	1210	1158	709	802	784	512	520	447	361	403	1018	441
	P62269	RPS18	981	1089	674	869	911	583	467	391	333	729	977	521
	P39019	RPS19	1122	1099	937	993	888	594	461	384	360	285	851	506
	P60866	RPS20	1123	968	858	736	995	472	424	226	365	293	701	544
	P63220	RPS21	1215	988	954	1036	718	653	704	340	444	549	502	614
	P62266	RPS23	1219	957	776	785	756	475	305	297	348	516	634	345
	P62847	RPS24	1017	1056	899	1073	890	652	496	409	290	484	779	486
	P62851	RPS25	1111	1211	1052	925	563	812	450	313	525	428	1066	410
	P62854	RPS26	975	1400	1428	885	1000	916	428	250			371	1242
	P42677	RPS27	1051	997	684	811	616	595	514	405	428	610	446	631
	P62979	RPS27A		710	451	1108	966	668	828	350	483	265	489	577
	P62857	RPS28	828	1106	802	809	917	596	557	367	401	598	726	391
	P62273	RPS29	1256	1064	1068	873	916	722	519	318	536	1056	702	365
	P62861	FAU(RPS30)	1265	981	675	1487	908	990	528	320	403	150	695	407
60S Subunit	P05388	RPLP0	1152	1066	662	1028	1146	711	690	821	564	731	1069	520
	P05386	RPLP1	526	732	650	1030	373	913	817	678	594	416	323	503
	P05387	RPLP2	908	733	476	766	929	666	575	481	686	260	302	401
	P39023	RPL3	830	665	524	1047	455	800	332	160	184	366	824	161
	P36578	RPL4	832	563	410	1247	633	891	317	302	207	459	758	246
	P46777	RPL5	873	638	566	841	853	1053	830	843	624	612	889	778
	Q02878	RPL6	701	562	478	1199	601	815	389	331	306	689	578	340
	P18124	RPL7	816	618	457	1057	739	789	354	227	137	157	716	305
	Q6DKI1	RPL7L1	1842		1483	41								
	P62424	RPL7A	929	775	582	1230	404	639	353	237	262	448	743	180
	P62917	RPL8	728	731	481	1266	504	773	333	246	153	234	757	303
	P32969	RPL9	1153	662	347	1334	368	806	318	195	265	595	870	291
	P27635	RPL10	960	789	668	1177	974	809	399	311	263	489	712	420
	P62906	RPL10A	808	621	360	1227	461	787	313	241	147	471	769	251
	P62913	RPL11	793	712	491	1326	1123	710	497	40	201	375	401	377
	P30050	RPL12	863	763	614	1208	305	814	338	321	254	314	845	286
	P26373	RPL13	836	530	492	1197	275	775	244	185	189	323	759	247
	P40429	RPL13A	737	940	375	1203	943	864	239	362	228	305	656	398
	P50914	RPL14	814	1136	561	1204	290	749	299	154	240	573	897	362
	P61313	RPL15	801	771	432	1246	556	820	388	244	205	360	841	353
	P18621	RPL17	799	1004	706	1170	610	350	308	315	209	518	597	166
	Q07020	RPL18	758	760	538	1229	369	971	248	368	269	422	754	314
	Q02543	RPL18A	847	484	551	1400	1285	830	437	328	232	304	605	289
	P84098	RPL19	1109	1118	651	1243	406	695	502	301	384	176	975	367
	P46778	RPL21	818	883	507	1161	647	836	382	319	247	607	509	139
	P35268	RPL22	729	714	450	474	515	306	52	42	347	1021	398	376
	P62829	RPL23	817	703	535	897	668	842	536	448	323	718	836	514
	P62750	RPL23A	1092	625	417	1146	844	807	162	222	165	458	753	358
	P83731	RPL24	1035	963	718	1141	643	743	421	307	299	139	1001	381
	P61254	RPL26	650	821	523	1160	664	636	192	229	320	547	649	279
	Q9UNX3	RPL26L1		1337		1693	454	567		122				
	P61353	RPL27	705	654	550	1158	614	925	301	192	326	430	941	216
	P46776	RPL27A	792	615	477	1151	295	901	306	274	211	105	599	182
	P46779	RPL28	666	566	412	1325	203	603	409	346	342	806	555	198
	P47914	RPL29	982	682	598	1219	660	660	303	235	346	615	847	294
	P62888	RPL30	621	659	570	1252	760	570	273	136	173	370	808	220
	P62899	RPL31	543	1026	590	1142	1104	811	567	286	376	379	568	336
	P62910	RPL32	885	583	416	1324	301	926	381	199	252	1055	910	242
	P49207	RPL34	1135	1410	350	1285	597	546	278	123	305	223	658	260
	P42766	RPL35	731	508	356	1058	518	593	175	168	104	67	454	128
	P18077	RPL35A	951	614	772	1366	814	840	385	219	193	255	813	102
	Q9Y3U8	RPL36	1157	845	317	1231	125	961	414	395	128	239	823	230
	P83881	RPL36A	1238								382	295	1511	
	Q969Q0	RPL36AL		1347	522	937	211	609	601	489				168
	P61927	RPL37	309				1012		458			1638	130	474
	P61513	RPL37A	1142	827	526	940	613	707	551	238	237	562	1075	162
	P63173	RPL38	780	1052	409	1046	387	623	280	210	266	555	586	264

Color Scale: Top 15% 15-30% 30-50% >50%

Figure 8. Ribosomal proteins in the 2nd-Z-rankings. The ranks of the ribosomal proteins in the 2nd-Z-rankings of the 12 NTRs are presented. The color scale is set by the percentile rank as indicated. For the 3rd-Z-rankings, see ***Supplementary file 11B***.

DOI: 10.7554/eLife.21184.016

13 reported cargo glucocorticoid receptor (**Tao et al., 2006**) in our MS, but proteins that may interact with nuclear receptors, e.g., thyroid hormone receptor-associated protein 3 (THRAP3) (**Ito et al., 1999**), RNA-binding protein 14 (RBM14) (**Iwasaki et al., 2001**), and transcription activator BRG1 (SMARCA4) (**Dai et al., 2008**), were identified as Imp-13 2nd-Z-15% cargoes. THRAP3 interacts with EJC (**Lee et al., 2010**), whose subunits, RNA-binding protein RBM8A and mago nashi homolog MAGOH, are well-characterized Imp-13 cargoes (**Mingot et al., 2001**). RBM8A and MAGOH are highly ranked Imp-13 3rd-Z-4% cargoes, which were not identified as cargoes of the other NTRs with the exception of Trn-1. However, another EJC subunit, that is, translation initiation factor 4A-III (EIF4A3) (**Shibuya et al., 2004**), was identified as an Imp-11 3rd-Z-4% cargo. Thus, the EJC subunits are imported through different pathways. A well-characterized Imp-13 cargo, SUMO-conjugating enzyme UBC9 (UBE2I) (**Mingot et al., 2001**), was identified as a 3rd-Z-4% cargo, and SUMO2 and SUMO3 were also identified as 3rd-Z-4% cargoes. Components of the chromatin accessibility complex CHRAC15 (CHRAC1) and DNA polymerase ε subunit 3 (POLE3) are also Imp-13 reported cargoes (**Walker et al., 2009**), and they are highly ranked 3rd-Z-4% cargoes. In the GO analysis, Imp-13 was linked to chromatin modification by the 2nd-Z-15% cargoes (**Supplementary file 6A**). Nucleolar complex protein 2 homolog (NOC2L) is ranked 10th in both the second and third Z-scores, and lysine-specific demethylase 2A (KDM2A) is ranked second in the second Z-score. The Imp-13 2nd-Z-15% cargoes include many actin-related proteins that are involved in chromatin remodeling and transcription (**Oma and Harata, 2011**; **Yoo et al., 2007**).

Surprisingly, a reported Imp-13 export cargo eIF1A (EIF1AX; **Mingot et al., 2001**) was identified as a 2nd-Z-15% cargo (ranked 84th and 164th by the second and third Z-score, respectively; **Supplementary files 1** and **3**). If a protein endogenous to the permeabilized cell nuclei is exported preferentially in the +NTR in vitro transport reaction, the $(L/H_{+NTR})/(L/H_{Ctl})$ value will be raised and the protein will be ranked high. However, it cannot be generalized because we have only one example. Most of the highly ranked Imp-13 cargoes must be import cargoes, because in all the bead halo assays where the cargoes bound to Imp-13 RanGTP inhibited the binding (**Supplementary file 2**).

Trn-SR cargoes

The reported Trn-SR cargoes include SR-rich splicing factors (SFs) that coordinate transcription elongation, mRNA splicing, and mRNA export (**Zhong et al., 2009**). Here, we found that proteins engaging in these processes are also Trn-SR cargoes. The Trn-SR 3rd-Z-4% cargoes include the RNA polymerase (RNAP) II elongation factors NELFE and PAF1 (a subunit of the Paf1 complex, PAF1C), DDX and DHX family RNA helicases, and the THO complex subunit THOC1 as well as SR-rich SFs. The 2nd-Z-15% cargoes additionally include PAF1C subunits CTR9, CDC73, and LEO, FACT complex subunits SSRP1 and SPT16, additional DDX and DHX family helicases, and THOC6 and THOC3 (**Supplementary file 5C and 5E**). Trn-SR bound to NELFE, CDC73, DDX5, and DDX27 in the bead halo assays (**Figure 3**, **Supplementary files 1**, **2,** and **3**). Peptidyl-prolyl cis-trans isomerases, which are contained in human spliceosomes (**Wahl et al., 2009**), were also identified as 3rd-Z-4% and 2nd-Z-15% cargoes. DnaJ homologs were also identified as 3rd-Z-4% and 2nd-Z-15% cargoes, although the spliceosome component DNAJC8 (**Zhou et al., 2002**) was not. The 3rd-Z-4% cargoes also include proteins related to nuclear division or chromosome segregation, the Ser/Thr protein kinase PLK1, dual specificity protein kinase TTK, G2/M-specific cyclin-B1 (CCNB1), cyclin-dependent kinase (CDK) 2, protein FAM83D, and dynein 1 light intermediate chain 1 (DYNC1LI1) in addition to proteins related to histone acetylation or deacetylation including histone deacetylase complex subunit SAP18 and SAGA-associated factor 29 homolog CCDC101. Indeed, in the bead halo assays, Trn-SR bound to SAP18 and CCDC101 (**Figure 3**; **Supplementary files 1**, **2,** and **3**). Additionally, the 2nd-Z-15% cargoes include many proteins that are related to nucleosome or chromatin regulation. Thus, the Trn-SR cargoes are involved in chromosome regulation in addition to the coordination of transcription elongation, mRNA splicing, and mRNA export.

Surprisingly, SR-rich SFs, which have been assumed to be Trn-SR-specific cargoes, were also identified as cargoes of other NTRs (**Figure 7**). To determine the allocation of the other SR-domain proteins to the NTRs, we here analyzed the distribution of SRSRSR hexa-peptide sequences in the 3rd-Z-4% cargoes (**Supplementary file 11E**). Imp-5, -7, -8, and Exp-4 as well as Trn-SR may be the specific NTRs for proteins with the hexa-peptide, most of which are nuclear proteins. The hexa-peptide-containing proteins other than the SR-rich SFs are primarily included in the Imp-5 and Exp-4 cargoes.

Imp-β cargoes

The Imp-β cargoes play roles in DNA synthesis and repair and chromatin regulation. The Imp-β 3rd-Z-4% cargoes include DNA polymerase δ subunits (POLD2 and 3) and mismatch repair endonuclease PMS2 (**Supplementary file 5C**). Additionally, the Imp-β 2nd-Z-15% cargoes include PCNA-associated factor KIAA0101 and DNA-(apurinic or apyrimidinic site) lyase (APEX1) (**Supplementary file 5E**). These proteins act in DNA synthesis or repair. The notable 3rd-Z-4% cargoes related to chromatin regulation include high-mobility group (HMG) proteins, histone acetyltransferase complex NuA4 subunit MRGBP, SWI/SNF-related regulator of chromatin SMARCE1, Spindlin-1 (SPIN1), chromodomain-helicase CHD8, and lymphoid-specific helicase HELLS. Additionally, the 2nd-Z-15% cargoes include the NuA4 subunit MORF4L2, SWI/SNF complex subunit SMARCC2, chromatin assembly factor 1 subunit CHAF1B, polycomb protein EED, and sister chromatid cohesion protein PDS5B. Chromatin remodeling by some of these factors is closely related to transcription. The 3rd-Z-4% cargoes include general transcription factor TFIIF (GTF2F1 and 2), TFIIH subunit MAT1, and TBP-associating factor TAF15, and the 2nd-Z-15% cargoes include TFIIH subunit cyclin-H (CCNH) and mediator complex subunit MED15. The sequence-specific transcription factors and cofactors are described above. mRNA capping factors are Imp-β cargoes as described. Thus, many Imp-β cargoes are related to the initial stage of gene expression.

Trn-1 and -2 cargoes

The transcription factor ATF1 was ranked first in both the 2nd- and 3rd-Z-rankings of the Trn-1 and -2 but was ranked low for the other NTRs (**Figure 3**; **Supplementary files 3** and **5**). As described, many of the cargoes that ranked higher in the Trn-1 and -2 2nd- and 3rd-Z-rankings (e.g. hnRNPs) are shared by Trn-1 and -2, but RPs are included only in the Trn-2 3rd-Z-4% cargoes. Additional divergences can be observed between their 2nd-Z-15% cargoes. As expected, their cargoes include many mRNA processing factors, but among them snRNPs are preferentially included in the Trn-2 2nd-Z-15% cargoes (**Figure 7**). Actin and actin-related proteins (ARPs), which play roles in chromatin remodeling and transcription (**Visa and Percipalle, 2010**; **Yoo et al., 2007**), proteins related to nuclear division, and tRNA ligases are preferentially Trn-1 cargoes, whereas proteins related to DNA repair and HMG proteins are preferentially Trn-2 cargoes (**Supplementary file 5E**).

Imp-4 cargoes

In the GO analysis, Imp-4 was linked to DNA metabolic processes, chromosome organization, and related terms (**Figures 5** and **6**). Consistently, replication factor C subunit 5 (RFC5) and HMG proteins are Imp-4 3rd-Z-4% cargoes, and the 2nd-Z-15% cargoes include DNA polymerase α subunit POLA1, DNA ligase I (LIG1), DNA topoisomerase I (TOP1), SWI/SNF complex subunit SMARCC2, the SWI/SNF-related chromatin regulator SMARCA5, nucleosome remodeling factor subunit BPTF, and FACT complex subunit SPT16 (**Supplementary file 5C and 5E**). The participation of the Imp-4 cargoes in chromatin organization is supported by a report that Imp-4 binds to the histone chaperon complex (**Tagami et al., 2004**), although the subunits were not identified in our MS. Imp-4 was also linked to cell cycle in the GO analysis. The Imp-4 3rd-Z-4% cargoes include the regulator of chromosome condensation RCC1 and the Ser/Thr protein kinase PLK1, and the 2nd-Z-15% cargoes include the sister chromatid cohesion protein PDS5 homolog PDS5B. Imp-4 was also linked to programed cell death or apoptosis in the GO analysis. The representative related 3rd-Z-4% cargoes are the death-promoting transcriptional repressor BCLAF1 and the tumor suppressor ARF (CDKN2A), and the 2nd-Z-15% cargoes are ribosomal L1 domain-containing protein 1 (RSL1D1) and apoptosis-inducing factor 1 (AIFM1).

Imp-5 cargoes

Few characteristics are unique to the Imp-5 3rd-Z-4% cargo cohort. However, this cohort includes proteins related to ribosome biogenesis, such as rRNA 2'-O-methyltransferase fibrillarin (FBL), H/ACA ribonucleoprotein complex subunit 1 (GAR1), and the ribosome biogenesis protein BOP1. This group also includes proteins related to nucleosome or chromatin organization, including spindlin-1 (SPIN1), protein DEK, the methyl-CpG-binding domain protein MBD2, and the paired amphipathic helix protein SIN3B (**Supplementary file 5C**). SR-rich SFs are also included as described. The Imp-5 2nd-Z-15% cargoes include many ARPs, proteins related to spindle organization or microtubule-

based processes, and several CDKs (**Supplementary file 5E**). Thus, a portion of the Imp-5 cargoes may be involved in cytokinesis. A number of translation initiation factors (eIFs) and elongation factors, many of which are annotated with nuclear localization (**Supplementary file 1**), are also among the Imp-5 2nd-Z-15% cargoes.

Imp-7 and -8 cargoes

The cognate NTRs Imp-7 and -8 share many 3rd-Z-4% and 2nd-Z-15% cargoes (**Figure 4**; **Supplementary file 5A**). The major cargoes of these NTRs are a range of mRNA SFs, but by the third Z-scores, snRNPs were identified only as Imp-7 and not Im-8 cargoes (**Supplementary file 5C**). Additional divergences can be observed between the Imp-7 and -8 cargoes (**Supplementary file 5C and 5E**). HMG proteins were identified only as Imp-7 3rd-Z-4% and 2nd-Z-15% cargoes, whereas more RPs were identified as Imp-8 cargoes. Proteins related to cell cycle regulation, the mitotic checkpoint protein BUB3, cell division cycle 5-like protein (CDC5L), and CDK12, are included in the Imp-7 3rd-Z-4% cargoes, and the Ser/Thr protein kinase PLK1 is a 2nd-Z-15% cargo, but these proteins are not Imp-8 cargoes. Many eIFs are Imp-8 but not Imp-7 2nd-Z-15% cargoes.

Imp-9 cargoes

The Imp-9 cargoes include many RPs and mRNA SFs. Proteins that are important for DNA packaging or nucleosome organization were also identified as Imp-9 cargoes (**Supplementary file 5C and 5E**). Histone H2A.Z, which is located in specific regions on chromosome (**Weber and Henikoff, 2014**), is ranked first and third in the third and second Z-scores, respectively. Additionally, the linker histone H1 (H1F0), histone-lysine N-methyltransferase 2A (KMT2A), and the SPT16 and SSRP1 subunits of the FACT complex, which regulates histone H2A.Z (**Jeronimo et al., 2015**), were also identified as 3rd-Z-4% cargoes. Among the Imp-9 2nd-Z-15% cargoes, other histones, DNA topoisomerase I (TOP1) and IIα (TOP2A), HMG proteins, SWI/SNF-related matrix-associated actin-dependent regulator of chromatin subfamily E member 1 (SMARCE1), and scaffold attachment factor B1 (SAFB) are included.

Imp-11 cargoes

Imp-11 was linked to developmental processes in the GO analysis (**Figure 5**; **Supplementary file 6A**), and few proteins with typical nuclear functions, such as DNA replication, nucleosome organization, and transcription, were found among the Imp-11 3rd-Z-4% cargoes (**Supplementary file 5C**). The Imp-11 2nd-Z-15% cargoes include several proteins related to nuclear division, such as Pogo transposable element with ZNF domain (POGZ), α-endosulfine (ENSA), CDK regulatory subunit 2 (CKS2), and the Ser/Thr protein kinase NEK7 (**Supplementary file 5E**). Many ARPs, tubulins and their related factors, tRNA ligases, and mRNA SFs are also in the Imp-11 2nd-Z-15% cargoes.

Exp-4 cargoes

The subunits of RNAP II elongation factors and mRNA processing factors are the representative Exp-4 cargoes, although they are also cargoes of several other NTRs (**Supplementary file 5C and 5E**). PAF1C subunit parafibromin (CDC73) is an Exp-4 3rd-Z-4% cargo, and other PAF1C subunits, that is, PAF1 and RTF1, FACT complex subunits, i.e., SSRP1 and SPT16 (SUPT16H), and elongation complex protein 2 (ELP2) are 2nd-Z-15% cargoes. A variety of mRNA processing factors, including 3'-end processing factors and THO complex subunits, are also Exp-4 3rd-Z-4% and 2nd-Z-15% cargoes. Thus, the factors that act in processes from transcription elongation to mRNA export are included in the Exp-4 cargoes. As discussed for another bi-directional NTR Imp-13, the possibility cannot be denied that the identified Exp-4 candidate cargoes include export cargoes.

Seemingly non-nuclear proteins

A number of nucleoporins (NUPs), which are the components of the NPC, were identified as cargoes. Increasing evidence demonstrates that the import of NUPs through NPCs is important for gene expression (**Burns and Wente, 2014**). Moreover, many mitochondrial proteins are highly ranked. These proteins preferentially localize to the mitochondria due to chaperon-regulated or cotranslational mechanisms in vivo and might interact with NTRs in the in vitro transport system. The transport system contains cytosolic extract and unlabeled (light) mitochondrial proteins in it could be

imported if they interact with NTRs. The $(L/H_{+NTR})/(L/H_{Ctl})$ values of them can be calculated, because LC-MS/MS can quantify low levels of labeled (heavy) proteins whether they are endogenous to the recipient nuclei or residual after washing. Thus, mitochondrial proteins with high $(L/H_{+NTR})/(L/H_{Ctl})$ values are imported proteins even if the import is fortuitous. Nuclear localization is annotated to many mitochondrial proteins (***Supplementary file 1***), and actual nuclear localization is possible as in the cases of AIFM1 and ATFS-1 (***Nargund et al., 2012***; ***Susin et al., 1999***). As was the case with the high-throughput cargo identification of the export receptor Exp-1 (CRM1) (***Kırlı et al., 2015***), our method identified other seemingly cytoplasmic proteins as cargoes. We did not detect direct binding between the NTRs and some of these cytoplasmic proteins, for example, Ras-related Rab family proteins and S100 proteins, in the bead halo assays (***Supplementary file 2***), but nuclear import by indirect binding is still possible.

Additional remarks

Here, we have presented the first complete picture of nuclear import via the 12 importin pathways. The 12 pathways must serve distinct roles because the NTRs are linked to different cellular processes by their cargoes. However, the cargoes are intricately allocated to the NTRs, and each NTR is linked to multiple cellular processes. The biological functions of NTRs designated in this work should be further clarified in future experiments.

We used HeLa nuclear extract as the cargo source, but it might not reconstitute all NTR–cargo interactions precisely because proteins in the nuclear extract might have different modifications or binding partners from those in cytoplasm where NTRs bind to cargoes in vivo. Some reported cargoes were ranked lower in the 2nd- and 3rd-Z-ranking, and it might be attributable to these differences of protein states. Alternatively, the transport capacity of our in vitro transport system might not be enough to identify all the cargoes, especially those with low transport efficiency. To reach a definitive conclusion, experiments in vivo might be needed.

We could not find any novel motifs that may serve as NTR-binding sites on the identified cargoes using the ungapped motif search method of MEME (***Bailey and Elkan, 1994***). A more extensive search for such motifs and higher order structures using alternative methods is currently underway.

Materials and methods

SILAC-Tp

SILAC-Tp has previously been described in detail (***Kimura et al., 2014***), but we provide a brief description here. HeLa-S3 cytosolic and nuclear extracts were depleted of Imp-β family NTRs with phenyl-Sepharose (GE healthcare), and the nuclear extract was subsequently depleted of RCC1 with a Ran-affinity method and concentrated. The extracts were dialyzed against transport buffer (TB, 20 mM HEPES–KOH (pH 7.3), 110 mM KOAc, 2 mM MgOAc, 5 mM NaOAc, 0.5 mM EGTA, 2 mM DTT, and 1 µg/mL each of aprotinin, pepstatin A, and leupeptin). Adherent HeLa-S3 cells were labeled with u-$^{13}C_6$ Lys and u-$^{13}C_6$ Arg by SILAC (***Ong et al., 2002***) and seeded onto a glass plate. After rinsing in ice cold TB, the cells were permeabilized with 40 µg/mL digitonin in TB for 5 min on ice and then rinsed again. The permeabilized cells were pretreated with 4 µM RanGDP and an ATP regeneration system in TB for 20 min at 30˚C to remove the residual Imp-β family NTRs and then rinsed. The cells were incubated in transport mixture (50% cytosolic extract, 10% nuclear extract, 1 µM p10/NTF2, and ATP regeneration system in TB) with (+NTR) or without (Ctl) 0.3–0.7 µM of one NTR for 20 min at 30˚C for the import reaction. (The NTR concentrations were optimized using the recombinant cargoes presented in ***Figure 1—figure supplement 1C***.) After rinsing, the cells were incubated in extract mixture (50% cytosolic extract and ATP regeneration system in TB) for 20 min at 30˚C and rinsed with NaCl-TB (TB containing 110 mM NaCl instead of KOAc) to remove the nonspecifically binding proteins. To extract the proteins, the cells were suspended in nuclear buffer (20 mM Tris–HCl, pH 8.0, 420 mM NaCl, 1.5 mM $MgCl_2$, 0.2 mM EDTA, 2 mM DTT, and 1 µg/mL each of aprotinin, pepstatin A, and leupeptin), sonicated, and centrifuged.

Actually, the transport reactions for two NTRs were simultaneously performed with one control reaction and triplicated. The simultaneously processed NTRs were Imp-β and Imp-13, Trn-1 and -2, Imp-7 and -8, Imp-9 and -11, and Imp-5 and Trn-SR, and the reactions for Imp-4 and Exp-4 were performed individually with controls.

Peptide analysis by LC-MS/MS

After the in vitro transport reaction, 25 µg each of the extracted proteins was concentrated by acetone precipitation, reduced with DTT, and alkylated with iodoacetamide. The proteins were digested with trypsin and Lys-C endopeptidase (enzyme/substrate ≈ 1/50) for 16 hr at 37°C. The peptides were evaporated to dryness, dissolved in Solvent-1 (0.1% TFA and 15% CH_3CN), and fractionated on Empore Cation Exchange-SR (3M, Maplewood, Minnesota). For the fractionation, the support was stacked manually inside the tapered end of a micropipette tip, the tip was fixed into the punched lid of a microtube, and the liquids were run by centrifugation (***Wiśniewski et al., 2009***). The resin was sequentially washed by ethanol and Solvent-1 containing 500 mM ammonium acetate and equilibrated with Solvent-1, and the peptides were then applied. After washing in Solvent-1, the peptides were eluted stepwise by Solvent-1 containing 125, 250, and 500 mM ammonium acetate and Solvent-2 (5% NH_4OH, 30% methanol, and 15% CH_3CN). The eluates were evaporated to dryness, and the peptides were dissolved in 0.1% TFA and 2% CH_3CN.

The peptides were applied to a liquid chromatograph (LC) (EASY-nLC 1000; Thermo Fisher Scientific, Waltham, Massachusetts) coupled to a Q Exactive hybrid quadrupole-Orbitrap mass spectrometer (Thermo Fisher Scientific) with a nanospray ion source in positive mode. The LC was performed on a NANO-HPLC capillary column C18 (75 µm x 150 mm, 3 µm particle size, Nikkyo Technos, Tokyo) at 45°C. The peptides were eluted with a 100-min 0–30% CH_3CN gradient and a subsequent 20-min 30–65% gradient in the presence of 0.1% formic acid at a flow rate of 300 nL/min. The Q Exactive-MS was operated in the top-10 data-dependent scan mode. The parameters for the Q Exactive operation were as follows: spray voltage, 2.3 kV; capillary temperature, 275°C; mass range (m/z), 350–1800; and normalized collision energy, 28%. The raw data were acquired with Xcalibur (RRID:SCR_014593; ver. 2.2 SP1).

Protein identification and quantitation

The MS and MS/MS data were searched against the Swiss-Prot database (2014_07–2016_01) using Proteome Discoverer (RRID:SCR_014477; ver. 1.4, Thermo Fisher Scientific) with the MASCOT search engine software (RRID:SCR_014322; ver. 2.4.1, Matrix Science, London). The search parameters were as follows: taxonomy, *Homo sapiens*; enzyme, trypsin; static modifications, carbamidomethyl (Cys); dynamic modifications, oxidation (Met); precursor mass tolerance, ±6 ppm; fragment mass tolerance, ±20 mDa; maximum missed cleavages, 1; and quantitation, SILAC (R6, K6). The proteins were considered identified when their false discovery rates were less than 5%. The SILAC L/H ratios were also calculated by Proteome Discoverer (ver. 1.4) with the default setting: show the raw quan values, false; minimum quan value threshold, 0; replace missing quan values with minimum intensity, false; use single-peak quan channels, false; apply quan value corrections, true; reject all quan values if not all quan channels are present, false; fold change threshold for up-/down-regulation, 1.5; maximum allowed fold change, 100; use ratios above maximum allowed fold change for quantification, false; percent co-isolation excluding peptides from quantification, 100; protein quantification, use only unique peptides; experimental bias, none. Proteins with L/H count ≥1 were included in further analysis. The L/H counts are shown in ***Supplementary file 1***. To access the mass spectrometry data, see below.

From the SILAC quantitation values of the control and +NTR reactions, the +NTR/Ctl = $(L/H_{+NTR})/(L/H_{Ctl})$ ratio of each protein was calculated, and the Z-score of the log_2(+NTR/Ctl) of each protein was calculated within each replicate.

$$Z-score=(X-\mu)/\sigma$$

where X is $log_2(+NTR/Ctl)=log_2[(L/H_{+NTR})/(L/H_{Ctl})]$ of each protein, μ is the mean of X, and σ is the standard deviation of X.

Reported cargo rate and recall

To calculate reported cargo rate (a lower bound on precision) and recall (sensitivity), we used the 27 and 25 reported cargoes of Trn-1 as the positive examples of the 2nd- and 3rd-Z-rankings, respectively. We do not have explicit labeling of negative examples. Most likely some portion of the proteins not reported as cargoes are genuine cargoes, but it is difficult to estimate that portion. Therefore, as a rough guide we tallied statistics under two simple assumptions: (i) that all proteins

not reported as cargoes should be treated as negative examples and (ii) that in the proteins not reported as cargoes, proteins annotated in Uniprot (RRID:SCR_002380) as having non-nuclear subcellular localization should be treated as negative examples and the other proteins excluded from the analysis (treated as neither positive nor negative). The first definition yielded 1622 and 1210 negative examples in the 2nd- and 3rd-Z-ranking, respectively, and the second definition 259 and 178 in the 2nd- and 3rd-Z-ranking, respectively. Since the first definition is maximally pessimistic, it allows estimation of an upper bound on the rate of false positives, while the second definition is more optimistic.

$$Reported\,cargo\,rate(i) = p(i)/[p(i) + n(i)]$$

$$Recall(i) = p(i)/P$$

where $p(i)$ denotes the number of previously reported cargoes (a lower bound on the number of positive examples) and $n(i)$ denotes the number of negative examples in the top i%; while P denotes the total number of previously reported cargoes.

Gene ontology analysis

GO (RRID:SCR_002811) analyses were performed using g:Profiler (RRID:SCR_006809; r1488-1536_e83_eg30) (**Reimand et al., 2016**). The search parameters were the following: organism, *Homo sapiens*; significance threshold, g:SCS; statistical domain size, all known genes; GO version, GO direct 2015-12-09 to 2016-01-21, releases/2015-12-08.

Phylogenetic analysis of the 12 Imp-β family NTRs

The phylogeny was inferred by maximum likelihood using RAxML (RRID:SCR_006086; ver. 8.1.17) (**Stamatakis, 2006**) with 1000 bootstrap replicates and the LG model with gamma-distributed rate variation. The amino acid sequences were aligned using Clustal Omega (RRID:SCR_001591; ver. 1.2.0) (**Sievers et al., 2011**) with the default parameters, and the resulting multiple alignments were trimmed using trimAl (ver. 1.2) (**Capella-Gutiérrez et al., 2009**) in gappyout mode.

Hierarchical clustering of the 11 Imp-β family NTRs based on the degree of overlap of the 3rd-Z-4% cargoes

We performed a hierarchical clustering of the Imp-β family NTRs based on their cargo profile similarities using Ward's method with Euclidean distance as implemented in the software R (RRID:SCR_001905; **R Development Core Team, 2012**). Here, we omitted Imp-β because its cargoes include many Imp-α-dependent indirect cargoes. To define a cargo profile for each NTR, we first defined a set of cargoes by merging the 3rd-Z-4% cargoes of the 11 NTRs other than Imp-β, which yielded a total of 426 cargoes. We then defined length 426 binary vectors for each NTR with a 1 for each cargo in the top 4% list and a 0 otherwise and input these 11 vectors into R to perform the clustering.

Bead halo assay

The proteins and *Escherichia coli* extracts were prepared as described (**Kimura et al., 2013a**). The bead halo assays (**Supplementary file 2**) were performed as described (**Patel and Rexach, 2008**). Briefly, GST or GST-NTR was immobilized on glutathione-Sepharose (GE healthcare), and mixed with an extract of *E. coli* expressing a GFP-fusion protein in EHBN buffer (10 mM EDTA, 0.5% 1,6-hexanediol, 10 mg/mL bovine serum albumin, and 125 mM NaCl), and the binding was observed by fluorescent microscopy. The GTP-fixed mutant of Ran Q69L-Ran, which inhibits specific NTR–cargo interactions, was added to determine the specificity of the binding. The expression and degradation levels of the GFP-fusion proteins were analyzed, and the concentrations of GFP-moieties were quantified by triplicate quantitative Western blotting of the extracts with an anti-GFP antibody. Because the GFP-moiety weakly bound to GST-Trn-1, GST-Trn-2, and GST-Trn-SR in the bead halo assay, the concentrations of the GFP-fusion proteins and GFP (control) were equalized, and images were acquired and processed under identical condition. In contrast, because the GFP-moiety does not bind to GST-Imp-13, GST-Imp-β, or GST-Imp-α, the control reaction mixture for these NTRs contained higher concentration of GFP than any other GFP-fusion proteins. Three images (GST, GST-

NTR, and GST-NTR + Q69L-Ran) for each GFP-fusion protein were acquired under identical conditions, and the background intensities and dynamic ranges were equalized.

Cell line

HeLa-S3 (RRID:CVCL_0058; mycoplasma, not detected) was obtained from Dr. Fumio Hanaoka (RIKEN).

Antibodies

See ***Supplementary file 12B***.

GFP-fusion proteins used for in vitro transport

The GFP-fusion proteins used in ***Figure 1—figure supplement 1C*** were prepared as described (***Kimura et al., 2013a***). For accessions and references, see ***Supplementary file 12B***. The SOX2 cDNA (pF1KB9652) was from Kazusa DNA Res. Inst. (Kisarazu, Japan), and the others were cloned from a HeLa cDNA library (SuperScript, Life Technology) by PCR.

Database deposition

The mass spectrometry proteomics data have been deposited to the ProteomeXchange Consortium (RRID:SCR_004055; http://www.proteomexchange.org/) via the PRIDE (RRID:SCR_003411; ***Vizcaíno et al., 2016***) partner repository with the dataset identifier PXD004655.

The .msf and .raw data files of each experiment summarized in ***Supplementary file 1*** are listed in ***Supplementary file 12A***. The protein and peptide quantitation results can be seen by opening .msf files by Proteome Discoverer software. To see spectra and chromatograms, .msf files and corresponding .raw files must be in the same local directory. A demo version of Proteome Discoverer can be downloaded at the Thermo Scientific omics software portal site (https://portal.thermo-brims.com/).

Acknowledgements

We thank Martin Beck, Alessandro Ori, and Kentaro Tomii for helpful discussion, Masahiro Oka for a supporting experiment, Shoko Motohashi and Ai Watanabe for technical assistance, and Hiroshi Mamada for a plasmid. We also thank the Support Unit for Bio-Material Analysis, RIKEN BSI Research Resource Center, especially Kaori Otsuki, Masaya Usui, and Aya Abe for MS analysis. This work was supported by JSPS KAKENHI Grant Number 15K07064 and a RIKEN FY2014 Incentive Research Project to MK, KAKENHI Grant Numbers 26251021, 26116526, and 15H05929 to NI, and the Platform Project for Supporting in Drug Discovery and Life Science Research (Platform for Drug Discovery, Informatics, and Structural Life Science) from the Japan Agency for Medical Research and Development (AMED) to KI.

Additional information

Funding

Funder	Grant reference number	Author
Japan Society for the Promotion of Science	KAKENHI,15K07064	Makoto Kimura
RIKEN	FY2014 Incentive Research Project	Makoto Kimura
Japan Agency for Medical Research and Development	Platform Project for Supporting in Drug Discovery and Life Science Research	Kenichiro Imai
Japan Society for the Promotion of Science	KAKENHI,26251021	Naoko Imamoto
Japan Society for the Promotion of Science	KAKENHI,26116526	Naoko Imamoto

Japan Society for the Promotion of Science	KAKENHI,15H05929	Naoko Imamoto

The funders had no role in study design, data collection and interpretation, or the decision to submit the work for publication.

Author contributions

MK, Conceptualization, Formal analysis, Funding acquisition, Investigation, Visualization, Methodology, Writing—original draft, Project administration, Writing—review and editing; YM, Formal analysis, Investigation, Visualization, Writing—review and editing; KI, Formal analysis, Funding acquisition, Investigation, Visualization, Methodology, Writing—review and editing; SK, Conceptualization, Resources, Methodology, Writing—review and editing; PH, Supervision, Validation, Investigation, Methodology, Writing—review and editing; NI, Conceptualization, Supervision, Funding acquisition, Validation, Project administration, Writing—review and editing

Author ORCIDs

Makoto Kimura, http://orcid.org/0000-0003-0868-5334
Naoko Imamoto, http://orcid.org/0000-0002-2886-3022

Additional files

Supplementary files

• Supplementary file 1. Results of SILAC-Tp. Each sheet contains the result of SILAC-Tp with one of the 12 NTRs. The proteins that exhibited $+NTR/Ctl = (L/H_{+NTR})/(L/H_{Ctl})$ values at least once in the three replicates (Experiments 1–3) are listed with the $\log_2[(\mathrm{L/H_{+NTR}})/(\mathrm{L/H_{Ctl}})]$ values. The second and third Z-scores and the ranks according to those scores are also presented. The 2nd-Z-15% and 3rd-Z-4% cargoes are indicated in cyan. The LC-MS/MS quantitation data for each replicate (Experiments 1–3) are also included. Light/Heavy, the median of quantified L/H values; Light/Heavy count, the number of quantified values; Light/Heavy variability, coefficient-of-variation for log-normal distributed data. [a]Report: The proteins listed by ***Chook and Süel (2011)*** are regarded as reported cargoes, and the references are provided in the Legend sheet. For Imp-β, only direct cargoes are listed. For Trn-2, the reported Trn-1 cargoes are listed. [b]Direct Binding: The results of the bead halo assays (***Supplementary file 2***) are summarized. ++ or +, positive; ± or –, negative. [c]GO Nucleus: Annotated with 'nucleus' in Gene Ontology (term type, cellular component). The rows can be sorted into preferable orders with Excel. To access the mass spectra, chromatograms, or raw data, see ***Supplementary file 12A***. Statistics: For each experiment, the number of proteins assigned with $\log_2[(\mathrm{L/H_{+NTR}})/(\mathrm{L/H_{Ctl}})]$ values (proteins assigned with Z-scores), the mean and standard deviation (S.D.) of $\log_2[(\mathrm{L/H_{+NTR}})/(\mathrm{L/H_{Ctl}})]$ are listed. $Z - score = (X - \mu)/\sigma$ where $X = \log_2[(\mathrm{L/H_{+NTR}})/(\mathrm{L/H_{Ctl}})]$ of each protein, μ is the mean of X in one experiment, and σ is the S.D. of X .

DOI: 10.7554/eLife.21184.017

• Supplementary file 2. NTR–cargo direct binding. The direct binding of the candidate cargoes to the NTRs was analyzed by bead halo assay. From well-characterized proteins that have not been reported as cargoes, (i) proteins ranked high (within the top 15% in the 2nd-Z-rankings or 4% in the 3rd-Z-rankings), around presumptive cutoffs (within about top 15–25% in the 2nd-Z-rankings), or lower and (ii) highly ranked proteins that are suspected as indirect cargoes or false positives based on their well-known features, e.g., PMPCA, GALE, UAP1, NQO2, EEF1A2, RAB2A, RAB8A, S100A4, S100A6, S100A13, and S100P, were selected and analyzed. Proteins in (i) verify the cargo identification and cutoff setting, and proteins in (ii) serve for finding indirect cargoes and false positives. The negative rate of these bead halo assays should be higher than the true overall false positive rate of the SILAC-Tp, because proteins in (ii) were selected preferentially. GST or GST-NTR was attached to glutathione-Sepharose beads, mixed with an extract of *E. coli* expressing GFP or a GFP-fusion protein, and observed by fluorescence microscopy. Q69L-Ran, which inhibits the NTR–cargo functional binding, was added as appropriate. The contrast of the bead fluorescence between the GST and GST-NTR indicates the binding, and the inhibition of this binding by Q69L-Ran certifies the specificity of the binding; ++ or +, positive; ± or –, negative. Summary of the results (p2–5): The results are

summarized in both 2nd- and 3rd-Z-rank order. The 2nd-Z-15% and 3rd-Z-4% cargoes are indicated by cyan, and positive binding (++ or +) is indicated by blue. Trn-1 (p6–8): The GFP-fusion proteins were divided into five groups (A–E) according to the expression levels. Because GFP binds weakly to Trn-1, the concentrations of GFP (control) and GFP-fusion proteins were equalized within each group, and the binding was observed in the same conditions. The images are comparable within a group. Trn-2 (p9): GFP weakly binds to Trn-2, and the concentrations of GFP and GFP-fusion proteins were equalized. The images are comparable. Proteins whose ranks differed substantially between the Trn-1 and Trn-2 Z-ranking were assayed. Imp-13 (p10–13): GFP does not bind to Imp-13, and GFP was added to the control mixture at the highest concentration. Three images (GST, GST-Imp-13, and GST-Imp-13 + Q69L-Ran) for each GFP-fusion protein were acquired under identical conditions, and the background intensities and dynamic ranges were equalized. Trn-SR (p14–16): GFP weakly binds to Trn-SR, and the procedures were similar to those used for Trn-1. The GFP-fusion proteins were divided into four groups (A–D), and the images are comparable within a group. Imp-**α**/*β* (p17–20): GFP does not bind to Imp-α or -*β*, and the procedures were similar to those used for Imp-13. GST-Imp-α_2 lacks the N-terminal Imp-*β*-binding domain. Western blotting (p21–22): The GFP-fusion proteins in the *E. coli* extracts were relatively quantified by Western blotting using an anti-GFP antibody (Roche). The extracts containing the amounts of protein (ng) indicated at the bottoms were loaded. The arrowheads indicate the expected full-length products. The GFP-moieties including those of the partial products were quantified by chemiluminescence. GFP was used as the standard. The Western blots were replicated more than three times. Accessions and sequences (p23–27): The cDNAs were cloned from a HeLa cDNA library by PCR. The accession numbers of the proteins are listed. If the sequence of a used protein is different from that in the database, the deleted, substituting, or inserted amino acids are indicated by the colors. The sequences that matched perfectly are not presented.

DOI: 10.7554/eLife.21184.018

• Supplementary file 3. The 2nd-Z-15% cargoes of the 12 NTRs. The 2nd-Z-15% cargoes of each NTR are listed by the gene names in the 2nd-Z-rank orders. The ranks by the third Z-scores are also shown. Cyan in the rank columns indicates the 2nd-Z-15% and 3rd-Z-4% cargoes. Colors in the gene name columns: magenta, reported cargoes; blue, cargoes bound directly to the NTR in the bead halo assays (***Supplementary file 2***); light blue, cargoes bound directly to Imp-α but not Imp-*β*; gray, proteins that did not bind to the NTRs; yellow, Imp-α; and green, reported export cargoes. For the 3rd-Z-4% cargoes, see ***Figure 3***.

DOI: 10.7554/eLife.21184.019

• Supplementary file 4. Example of extracted ion chromatograms (EICs) of peptides. EICs of GLUD1 peptides in the SILAC-Tp with Trn-1: As a general problem of high-throughput LC-MS/MS quantitation, quantitative values of proteins with fewer quantified peptides deviate among the replicates. Referring to EICs of the quantified peptides is useful to avoid misidentification of cargoes. For example, the L/H ratios of a Trn-1 2nd-Z-15% cargo GLUD1 (P00367, ranked 110th and 342nd by the second and third Z-score, respectively) deviated largely in the three replicates of SILAC-Tp with Trn-1 (***Supplementary file 1***). Panels (A–H) show EICs of the indicated peptide (trypsin targets, K and R, are written in lower cases) in the three (three Ctl and there +Trn) experiments (some peptides were not identified in all the experiments). Magenta letters indicate the quantified peptides and L/H rations. In panel (A), the elution time of the peptide TAMkYNLGLDLr differs largely between the expriment-1 Ctl and experiment-2 +Trn-1, the peak shape of the experiment-2 +Trn-1 is irregular, and the L/H ratio of it is much higher than those of other peptides in +Trn-1 experiments (B and E). Thus, there is concern about misidentification. Because the L/H count of GLUD1 in the experiment-2 +Trn-1 is two (TAMkYNLGLDLr and NLNHVSYGr, A and B) and the L/H ratio of a protein is defined as the median, the L/H ratio of GLUD1 in the expriment-2 +Trn-1 is affected by the L/H ratio of TAMkYNLGLDLr. Exclusion of the L/H ratio of TAMkYNLGLDLr in the experiment-2 +Trn-1 lowers the Z-score rank of GLUD1 significantly. In panel (C), the chromatogram of the peptide HGGTIPIVPTAEFQDr in the experiment-1 Ctl has an irregular peak, and the L/H ratio of it is much higher than those of other peptides in the Ctl experiments (A–H). Thus, overlap with other peptide or other failures may be possible. However, the L/H count of GLUD1 in the experiment-1 Ctl is four (TAMkYNLGLDLr, HGGTIPIVPTAEFQDr, ALASLMTYk, and GASIVEDkLVEDLr) and the value of HGGTIPIVPTAEFQDr does not affect the median. (The L/H ratio of TAMkYNLGLDLr, whose EIC

differ between the experiment-1 Ctl and expriment-2 +Trn in (A) as mentioned above, may affect the L/H ratio of GLUD1 in the experiment-1 Ctl, but we assumed that it is reliable.) As above, the L/H ratios of proteins with low L/H counts (***Supplementary file 1***) may be affected by LC-MS/MS artifacts, and misidentification can be avoided by referring to the EICs. All the EICs and MS spectra in this work can be accessed by downloading the mass spectrometry data and Proteome Discoverer software (see the Materials and methods and ***Supplementary file 12A***).

DOI: 10.7554/eLife.21184.020

• Supplementary file 5. Redundancy of NTRs: Cargoes shared by NTRs. (A) The numbers of the 2nd-Z-15% cargoes shared by two NTRs. For the 3rd-Z-4% cargoes, see ***Figure 4***. (B) Redundancy of the 3rd-Z-4% cargoes. Many proteins are included in the 3rd-Z-4% cargoes of multiple NTRs. The ranks of these cargoes in the 3rd-Z-rankings for all 12 NTRs are presented. (C) Relationships between the NTRs and the characteristics of their 3rd-Z-4% cargo proteins. The 3rd-Z-4% cargoes are grouped according to their characteristics (functions or biological processes that the proteins act in), and their ranks are presented as in (B). To make our points clear, typical terms for the protein characteristics and typical proteins related to the terms have been selected with reference to Gene Ontology (GO) and UniProt. Thus, the terms in this sheet are slightly different from those in the databases, fewer proteins than annotated in the databases are grouped, and the list is redundant. For the complete linkages between the GO terms and the 3rd-Z-4% cargoes, see ***Supplementary file 7***. (D) Redundancy of the 2nd-Z-15% cargoes. The ranks of the 2nd-Z-15% cargoes are presented as in (B). (E) Relationships between the NTRs and the characteristics of their 2rd-Z-15% cargo proteins. The 2nd-Z-15% cargoes are grouped, and their ranks are presented in a manner similar to that in (C). For the complete linkages between the GO terms and the 2nd-Z-15% cargoes, see ***Supplementary file 8***.

DOI: 10.7554/eLife.21184.021

• Supplementary file 6. GO term enrichments of the identified cargoes. (A) Extraction of the GO term enrichments of the 2nd-Z-15% cargoes. The 2nd-Z-15% cargoes were analyzed for GO term enrichment in (C). The terms that were significantly enriched ($p<0.05$, cyan) in the 2nd-Z-15% cargoes of four or fewer NTRs were selected, and terms that represent many similar terms are presented. With the p-values, the numbers (#) of cargoes annotated with each of the terms are presented. Total No. represents the number of proteins annotated with each term in the database. Related terms are bundled in the same color. For the 3rd-Z-4% cargoes, see ***Figures 5*** and ***6***. The correspondences between each 2nd-Z-15% cargo and GO term are summarized in ***Supplementary file 10***. All the GO terms annotated to the 2nd-Z-15% cargoes are listed in ***Supplementary file 8***. (B) Full table of the GO term enrichments of the 3rd-Z-4% cargoes. The 3rd-Z-4% cargoes were analyzed for GO term enrichment. For all combinations of GO terms and NTRs, the p-values for the term enrichments in the 3rd-Z-4% cargoes and the numbers (#) of cargoes annotated with the terms are presented. The numbers following '# in' are the total numbers of 3rd-Z-4% cargoes. Total No. represents the number of proteins annotated with each term in the database. Cyan, $p<0.05$. ***Figures 5*** and ***6*** were extracted from this table. This table was derived from ***Supplementary file 7***, and see ***Supplementary file 7*** to retrieve the protein accessions. (C) Full table of the GO term enrichments of the 2nd-Z-15% cargoes. The 2nd-Z-15% cargoes were analyzed and are presented in a manner similar to that in (B). (A) was extracted from this table. This table was derived from ***Supplementary file 8***, and see ***Supplementary file 8*** to retrieve the protein accessions.

DOI: 10.7554/eLife.21184.022

• Supplementary file 7. The 3rd-Z-4% cargoes annotated with GO terms. With respect to each NTR, the accessions of the 3rd-Z-4% cargoes annotated with each GO term are listed. Cyan, significant term enrichment ($p<0.05$) in the 3rd-Z-4% cargoes of the NTR. Total No. represents the number of proteins annotated with each term in the database. ***Supplementary files 6B*** and ***9*** were derived from this table. For the 2nd-Z-15% cargoes, see ***Supplementary file 8***.

DOI: 10.7554/eLife.21184.023

• Supplementary file 8. The 2nd-Z-15% cargoes annotated with GO terms. With respect to each NTR, the accessions of the 2nd-Z-15% cargoes annotated with each GO term are listed. Cyan, significant term enrichment ($p<0.05$) in the 2nd-Z-15% cargoes of the NTR. Total No. represents the number of proteins annotated with each term in the database. ***Supplementary files 6C*** and ***10*** were derived from this table. For the 3nd-Z-4% cargoes, see ***Supplementary file 7***.

DOI: 10.7554/eLife.21184.024

• Supplementary file 9. Correspondences between the 3rd-Z-4% cargoes and GO terms. Each sheet shows the correspondences between the 3rd-Z-4% cargoes of one NTR and selected GO terms. A term annotation to a cargo is indicated by '1' in the corresponding cell. Reported cargoes are indicated by magenta in the gene name cells, and the results of the bead halo assays (***Supplementary file 2***) are also indicated by colors in the gene name cells: blue, cargoes directly bound to the NTR; light blue, cargoes directly bound to Imp-α but not Imp-β; gray, proteins that did not bind to the NTR. GO terms that represent many similar terms were selected from the terms enriched significantly ($p<0.05$) for the 3rd-Z-4% cargoes of each NTR, and broadly defined terms were deselected. Magenta and orange in the term ID cells indicate terms that are significantly enriched for the cargoes of four or fewer NTRs, and of them magenta indicates the terms presented in ***Figures 5*** and ***6***. Related GO terms are bundled in the same color, and different colors are used to distinguish the columns easily. The NTRs added in the transport reactions (white in the rank cells) were not analyzed. This table was derived from ***Supplementary file 7***. For 2nd-Z-15% cargoes, see ***Supplementary file 10***.

DOI: 10.7554/eLife.21184.025

• Supplementary file 10. Correspondences between the 2nd-Z-15% cargoes and GO terms. Each sheet shows the correspondences between the 2nd-Z-15% cargoes of one NTR and selected GO terms. A term annotation to a cargo is indicated by '1' in the corresponding cell. Reported cargoes are indicated by magenta in the gene name cells, and the results of the bead halo assays (***Supplementary file 2***) are also indicated by colors in the gene name cells: blue, cargoes directly bound to the NTR; light blue, cargoes directly bond to Imp-α but not Imp-β; gray, proteins that did not bind to the NTR. GO terms that represent many similar terms were selected from the terms enriched significantly ($p<0.05$) for the 2nd-Z-15% cargoes of each NTR, and broadly defined terms were deselected. Magenta and orange in the term ID cells indicate terms that are significantly enriched for the cargoes of four or fewer NTRs, and of them magenta indicates the terms presented in ***Supplementary file 6A***. Related GO terms are bundled in the same color, and different colors are used to distinguish the columns easily. The NTRs added in the transport reactions (white in the rank cells) were not analyzed. This table was derived from ***Supplementary file 8***. For 3rd-Z-4% cargoes, see ***Supplementary file 9***.

DOI: 10.7554/eLife.21184.026

• Supplementary file 11. mRNA processing factors, ribosomal proteins, and transcription factors. (A) Ranks of mRNA processing factors. All of the 2nd-Z-15% and 3rd-Z-4% cargoes that are annotated with mRNA processing in Gene Ontology (GO) are listed with the ranks in the 2nd- and 3rd-Z-rankings. The color scale is set by percentile rank as indicated. ***Figure 7*** was extracted from this table. (B) The 3rd-Z-rankings of ribosomal proteins. The ranks of the ribosomal proteins in the 3rd-Z-rankings of the 12 NTRs are presented. The color scale is set by percentile rank as indicated. For the 2nd-Z-rankings, see ***Figure 8***. (C) Extracts of the GO term enrichments of the transcription factors found in the 2nd-Z-15% cargoes. Seventeen to 36 proteins in the 2nd-Z-15% cargoes of each NTR are annotated with 'transcription factor activity, sequence-specific DNA binding' or 'transcription factor activity, protein binding' in GO. The factors were analyzed for GO term enrichment (term type, biological process, BP) in (D). Typical terms that represent similar terms were extracted from (D). The p-value for the term enrichment and the number (#) of factors annotated with the term are presented. Total No. represents the number of proteins annotated with each term in the database. Cyan, $p<0.05$. Related terms are bundled in the same color. (D) Full table of the GO term enrichments of the transcription factors found in the 2nd-Z-15% cargoes. The 2nd-Z-15% cargoes that are annotated with 'transcription factor activity, sequence-specific DNA binding" or 'transcription factor activity, protein binding' in GO were analyzed for GO term enrichment (term type, BP). The analyzed transcription factors are listed at the bottom. For all of the combinations of GO terms and NTRs, the p-value for the term enrichment and the number (#) of transcription factors annotated with the term are presented. The numbers following '# in' are the total numbers of transcription factors in the 2nd-Z-15% cargoes. Total No. represents the number of proteins annotated with each term in the database. Cyan, $p<0.05$. (C) was extracted from this table. (E) SRSRSR motif in the 3rd-Z-4% cargoes. The 3rd-Z-4% cargoes that contain an 'SRSRSR' hexa-peptide sequence were counted.

DOI: 10.7554/eLife.21184.027

• Supplementary file 12. MS data files, recombinant cargoes, and antibodies. (A) MS data files. The mass spectrometry proteomics data (.msf and .raw files) have been deposited to the ProteomeXchange Consortium (http://www.proteomexchange.org/) with the dataset identifier PXD004655. The results of protein and peptide identification and quantitation are summarized in Supplementary file 1, and the .msf and .raw data files corresponding to each experiment in Supplementary file 1 are listed in this table. The quantitation results can be seen by opening .msf files by Proteome Discoverer software. To see spectra and chromatograms, .msf files and corresponding .raw files must be in the same local directory. A demo version of Proteome Discoverer can be downloaded at the Thermo Scientific omics software portal site (https://portal.thermo-brims.com/). (B) GFP-fusion proteins used for in vitro transport and antibodies.

DOI: 10.7554/eLife.21184.028

Major datasets

The following dataset was generated:

Author(s)	Year	Dataset title	Dataset URL	Database, license, and accessibility information
Kimura M, Imamoto N	2016	SILAC-Tp (12 importins)	http://www.ebi.ac.uk/pride/archive/projects/PXD004655	Publicly available at the Pride Archive (accession no: PXD004655)

References

Adam SA, Marr RS, Gerace L. 1990. Nuclear protein import in permeabilized mammalian cells requires soluble cytoplasmic factors. *The Journal of Cell Biology* **111**:807–816. doi: 10.1083/jcb.111.3.807, PMID: 2391365

Bailey TL, Elkan C. 1994. Fitting a mixture model by expectation maximization to discover motifs in biopolymers. *Proceedings of the Second International Conference on Intelligent Systems for Molecular Biology*:AAAI Press. p 28–36.

Beauchamp P, Nassif C, Hillock S, van der Giessen K, von Roretz C, Jasmin BJ, Gallouzi IE. 2010. The cleavage of HuR interferes with its transportin-2-mediated nuclear import and promotes muscle fiber formation. *Cell Death and Differentiation* **17**:1588–1599. doi: 10.1038/cdd.2010.34, PMID: 20379198

Bischoff FR, Ponstingl H. 1995. Catalysis of guanine nucleotide exchange of ran by RCC1 and stimulation of hydrolysis of Ran-bound GTP by Ran-GAP1. *Methods in Enzymology* **257**:135–144. doi: 10.1016/s0076-6879(95)57019-5, PMID: 8583915

Burns LT, Wente SR. 2014. From hypothesis to mechanism: uncovering nuclear pore complex links to gene expression. *Molecular and Cellular Biology* **34**:2114–2120. doi: 10.1128/MCB.01730-13, PMID: 24615017

Capella-Gutiérrez S, Silla-Martínez JM, Gabaldón T. 2009. trimAl: a tool for automated alignment trimming in large-scale phylogenetic analyses. *Bioinformatics* **25**:1972–1973. doi: 10.1093/bioinformatics/btp348, PMID: 19505945

Chook YM, Süel KE. 2011. Nuclear import by karyopherin-βs: recognition and inhibition. *Biochimica et Biophysica Acta (BBA) - Molecular Cell Research* **1813**:1593–1606. doi: 10.1016/j.bbamcr.2010.10.014, PMID: 21029754

Dai Y, Ngo D, Jacob J, Forman LW, Faller DV. 2008. Prohibitin and the SWI/SNF ATPase subunit BRG1 are required for effective androgen antagonist-mediated transcriptional repression of androgen receptor-regulated genes. *Carcinogenesis* **29**:1725–1733. doi: 10.1093/carcin/bgn117, PMID: 18487222

Gene Ontology Consortium. 2015. Gene Ontology Consortium: going forward. *Nucleic acids research* **43**: D1049–1056. doi: 10.1093/nar/gku1179, PMID: 25428369

Goldfarb DS, Corbett AH, Mason DA, Harreman MT, Adam SA. 2004. Importin alpha: a multipurpose nuclear-transport receptor. *Trends in Cell Biology* **14**:505–514. doi: 10.1016/j.tcb.2004.07.016, PMID: 15350979

Golomb L, Bublik DR, Wilder S, Nevo R, Kiss V, Grabusic K, Volarevic S, Oren M. 2012. Importin 7 and Exportin 1 link c-Myc and p53 to regulation of ribosomal biogenesis. *Molecular Cell* **45**:222–232. doi: 10.1016/j.molcel.2011.11.022, PMID: 22284678

Görlich D, Kutay U. 1999. Transport between the cell nucleus and the cytoplasm. *Annual Review of Cell and Developmental Biology* **15**:607–660. doi: 10.1146/annurev.cellbio.15.1.607, PMID: 10611974

Huang JG, Yang M, Liu P, Yang GD, Wu CA, Zheng CC. 2010. Genome-wide profiling of developmental, hormonal or environmental responsiveness of the nucleocytoplasmic transport receptors in Arabidopsis. *Gene* **451**:38–44. doi: 10.1016/j.gene.2009.11.009, PMID: 19944133

Hutten S, Kehlenbach RH. 2007. CRM1-mediated nuclear export: to the pore and beyond. *Trends in Cell Biology* **17**:193–201. doi: 10.1016/j.tcb.2007.02.003, PMID: 17317185

Ito M, Yuan CX, Malik S, Gu W, Fondell JD, Yamamura S, Fu ZY, Zhang X, Qin J, Roeder RG. 1999. Identity between TRAP and SMCC complexes indicates novel pathways for the function of nuclear receptors and

diverse mammalian activators. *Molecular Cell* **3**:361–370. doi: 10.1016/S1097-2765(00)80463-3, PMID: 10198638

Iwasaki T, Chin WW, Ko L. 2001. Identification and characterization of RRM-containing coactivator activator (CoAA) as TRBP-interacting protein, and its splice variant as a coactivator modulator (CoAM). *Journal of Biological Chemistry* **276**:33375–33383. doi: 10.1074/jbc.M101517200, PMID: 11443112

Jäkel S, Görlich D. 1998. Importin beta, transportin, RanBP5 and RanBP7 mediate nuclear import of ribosomal proteins in mammalian cells. *The EMBO Journal* **17**:4491–4502. doi: 10.1093/emboj/17.15.4491, PMID: 9687515

Jäkel S, Mingot JM, Schwarzmaier P, Hartmann E, Görlich D. 2002. Importins fulfil a dual function as nuclear import receptors and cytoplasmic chaperones for exposed basic domains. *The EMBO Journal* **21**:377–386. doi: 10.1093/emboj/21.3.377, PMID: 11823430

Jeronimo C, Watanabe S, Kaplan CD, Peterson CL, Robert F. 2015. The histone chaperones FACT and Spt6 restrict H2A.Z from intragenic locations. *Molecular Cell* **58**:1113–1123. doi: 10.1016/j.molcel.2015.03.030, PMID: 25959393

Kırlı K, Karaca S, Dehne HJ, Samwer M, Pan KT, Lenz C, Urlaub H, Görlich D. 2015. A deep proteomics perspective on CRM1-mediated nuclear export and nucleocytoplasmic partitioning. *eLife* **4**:e11466. doi: 10.7554/eLife.11466, PMID: 26673895

Kahle J, Baake M, Doenecke D, Albig W. 2005. Subunits of the heterotrimeric transcription factor NF-Y are imported into the nucleus by distinct pathways involving importin beta and importin 13. *Molecular and Cellular Biology* **25**:5339–5354. doi: 10.1128/MCB.25.13.5339-5354.2005, PMID: 15964792

Kang HS, Ock J, Lee HJ, Lee YJ, Kwon BM, Hong SH. 2013. Early growth response protein 1 upregulation and nuclear translocation by 2′-benzoyloxycinnamaldehyde induces prostate cancer cell death. *Cancer Letters* **329**:217–227. doi: 10.1016/j.canlet.2012.11.006, PMID: 23178451

Kataoka N, Bachorik JL, Dreyfuss G. 1999. Transportin-SR, a nuclear import receptor for SR proteins. *The Journal of Cell Biology* **145**:1145–1152. doi: 10.1083/jcb.145.6.1145, PMID: 10366588

Kimura M, Imamoto N. 2014. Biological significance of the importin-β family-dependent nucleocytoplasmic transport pathways. *Traffic* **15**:727–748. doi: 10.1111/tra.12174, PMID: 24766099

Kimura M, Kose S, Okumura N, Imai K, Furuta M, Sakiyama N, Tomii K, Horton P, Takao T, Imamoto N. 2013a. Identification of cargo proteins specific for the nucleocytoplasmic transport carrier transportin by combination of an in vitro transport system and stable isotope labeling by amino acids in cell culture (SILAC)-based quantitative proteomics. *Molecular & Cellular Proteomics* **12**:145–157. doi: 10.1074/mcp.M112.019414, PMID: 23087160

Kimura M, Okumura N, Kose S, Takao T, Imamoto N. 2013b. Identification of cargo proteins specific for importin-β with importin-α applying a stable isotope labeling by amino acids in cell culture (SILAC)-based in vitro transport system. *Journal of Biological Chemistry* **288**:24540–24549. doi: 10.1074/jbc.M113.489286, PMID: 23846694

Kimura M, Thakar K, Karaca S, Imamoto N, Kehlenbach RH. 2014. Novel approaches for the identification of nuclear transport receptor substrates. *Methods in Cell Biology* **122**:353–378. doi: 10.1016/B978-0-12-417160-2.00016-3, PMID: 24857738

Kobayashi J, Hirano H, Matsuura Y. 2015. Crystal structure of the karyopherin Kap121p bound to the extreme C-terminus of the protein phosphatase Cdc14p. *Biochemical and Biophysical Research Communications* **463**:309–314. doi: 10.1016/j.bbrc.2015.05.060, PMID: 26022122

Kobayashi J, Matsuura Y. 2013. Structural basis for cell-cycle-dependent nuclear import mediated by the karyopherin Kap121p. *Journal of Molecular Biology* **425**:1852–1868. doi: 10.1016/j.jmb.2013.02.035, PMID: 23541588

Kose S, Furuta M, Imamoto N. 2012. Hikeshi, a nuclear import carrier for Hsp70s, protects cells from heat shock-induced nuclear damage. *Cell* **149**:578–589. doi: 10.1016/j.cell.2012.02.058, PMID: 22541429

Lange A, Mills RE, Lange CJ, Stewart M, Devine SE, Corbett AH. 2007. Classical nuclear localization signals: definition, function, and interaction with importin alpha. *Journal of Biological Chemistry* **282**:5101–5105. doi: 10.1074/jbc.R600026200, PMID: 17170104

Lee BJ, Cansizoglu AE, Süel KE, Louis TH, Zhang Z, Chook YM. 2006. Rules for nuclear localization sequence recognition by Karyopherin Beta 2. *Cell* **126**:543–558. doi: 10.1016/j.cell.2006.05.049, PMID: 16901787

Lee KM, Hsu I, Tarn WY. 2010. TRAP150 activates pre-mRNA splicing and promotes nuclear mRNA degradation. *Nucleic Acids Research* **38**:3340–3350. doi: 10.1093/nar/gkq017, PMID: 20123736

Li KK, Yang L, Pang JC, Chan AK, Zhou L, Mao Y, Wang Y, Lau KM, Poon WS, Shi Z, Ng HK. 2013. MIR-137 suppresses growth and invasion, is downregulated in oligodendroglial tumors and targets CSE1L. *Brain Pathology* **23**:426–439. doi: 10.1111/bpa.12015, PMID: 23252729

Lieu KG, Shim EH, Wang J, Lokareddy RK, Tao T, Cingolani G, Zambetti GP, Jans DA. 2014. The p53-induced factor Ei24 inhibits nuclear import through an importin β-binding-like domain. *The Journal of Cell Biology* **205**:301–312. doi: 10.1083/jcb.201304055, PMID: 24821838

Lu M, Zak J, Chen S, Sanchez-Pulido L, Severson DT, Endicott J, Ponting CP, Schofield CJ, Lu X. 2014. A code for RanGDP binding in ankyrin repeats defines a nuclear import pathway. *Cell* **157**:1130–1145. doi: 10.1016/j.cell.2014.05.006, PMID: 24855949

Maertens GN, Cook NJ, Wang W, Hare S, Gupta SS, Öztop I, Lee K, Pye VE, Cosnefroy O, Snijders AP, KewalRamani VN, Fassati A, Engelman A, Cherepanov P. 2014. Structural basis for nuclear import of splicing factors by human Transportin 3. *PNAS* **111**:2728–2733. doi: 10.1073/pnas.1320755111, PMID: 24449914

Major AT, Whiley PA, Loveland KL. 2011. Expression of nucleocytoplasmic transport machinery: clues to regulation of spermatogenic development. *Biochimica et Biophysica Acta (BBA) - Molecular Cell Research* **1813**:1668–1688. doi: 10.1016/j.bbamcr.2011.03.008, PMID: 21420444

Makhnevych T, Lusk CP, Anderson AM, Aitchison JD, Wozniak RW. 2003. Cell cycle regulated transport controlled by alterations in the nuclear pore complex. *Cell* **115**:813–823. doi: 10.1016/S0092-8674(03)00986-3, PMID: 14697200

Mingot JM, Kostka S, Kraft R, Hartmann E, Görlich D. 2001. Importin 13: a novel mediator of nuclear import and export. *The EMBO Journal* **20**:3685–3694. doi: 10.1093/emboj/20.14.3685, PMID: 11447110

Nargund AM, Pellegrino MW, Fiorese CJ, Baker BM, Haynes CM. 2012. Mitochondrial import efficiency of ATFS-1 regulates mitochondrial UPR activation. *Science* **337**:587–590. doi: 10.1126/science.1223560, PMID: 22700657

Oma Y, Harata M. 2011. Actin-related proteins localized in the nucleus: from discovery to novel roles in nuclear organization. *Nucleus* **2**:38–46. doi: 10.4161/nucl.2.1.14510, PMID: 21647298

Ong SE, Blagoev B, Kratchmarova I, Kristensen DB, Steen H, Pandey A, Mann M. 2002. Stable isotope labeling by amino acids in cell culture, SILAC, as a simple and accurate approach to expression proteomics. *Molecular & Cellular Proteomics* **1**:376–386. doi: 10.1074/mcp.M200025-MCP200, PMID: 12118079

Patel SS, Rexach MF. 2008. Discovering novel interactions at the nuclear pore complex using bead halo: a rapid method for detecting molecular interactions of high and low affinity at equilibrium. *Molecular & Cellular Proteomics* **7**:121–131. doi: 10.1074/mcp.M700407-MCP200, PMID: 17897934

Perry RB, Fainzilber M. 2009. Nuclear transport factors in neuronal function. *Seminars in Cell & Developmental Biology* **20**:600–606. doi: 10.1016/j.semcdb.2009.04.014, PMID: 19409503

Pollard VW, Michael WM, Nakielny S, Siomi MC, Wang F, Dreyfuss G. 1996. A novel receptor-mediated nuclear protein import pathway. *Cell* **86**:985–994. doi: 10.1016/S0092-8674(00)80173-7, PMID: 8808633

Quan Y, Ji ZL, Wang X, Tartakoff AM, Tao T. 2008. Evolutionary and transcriptional analysis of karyopherin beta superfamily proteins. *Molecular & Cellular Proteomics* **7**:1254–1269. doi: 10.1074/mcp.M700511-MCP200, PMID: 18353765

R Development Core Team. 2012. R: A Language and environment for statistical computing. Vienna, Austria: R Foundation for Statistical Computing. http://www.R-project.org/

Rebane A, Aab A, Steitz JA. 2004. Transportins 1 and 2 are redundant nuclear import factors for hnRNP A1 and HuR. *RNA* **10**:590–599. doi: 10.1261/rna.5224304, PMID: 15037768

Reimand J, Arak T, Adler P, Kolberg L, Reisberg S, Peterson H, Vilo J. 2016. G:Profiler-a web server for functional interpretation of gene lists (2016 update). *Nucleic Acids Research* **44**:W83–W89. doi: 10.1093/nar/gkw199, PMID: 27098042

Rolland T, Taşan M, Charloteaux B, Pevzner SJ, Zhong Q, Sahni N, Yi S, Lemmens I, Fontanillo C, Mosca R, Kamburov A, Ghiassian SD, Yang X, Ghamsari L, Balcha D, Begg BE, Braun P, Brehme M, Broly MP, Carvunis AR, et al. 2014. A proteome-scale map of the human interactome network. *Cell* **159**:1212–1226. doi: 10.1016/j.cell.2014.10.050, PMID: 25416956

Schmidt HB, Görlich D. 2016. Transport Selectivity of nuclear pores, Phase Separation, and Membraneless Organelles. *Trends in Biochemical Sciences* **41**:46–61. doi: 10.1016/j.tibs.2015.11.001, PMID: 26705895

Shibuya T, Tange TØ, Sonenberg N, Moore MJ. 2004. eIF4AIII binds spliced mRNA in the exon junction complex and is essential for nonsense-mediated decay. *Nature Structural & Molecular Biology* **11**:346–351. doi: 10.1038/nsmb750, PMID: 15034551

Sievers F, Wilm A, Dineen D, Gibson TJ, Karplus K, Li W, Lopez R, McWilliam H, Remmert M, Söding J, Thompson JD, Higgins DG. 2011. Fast, scalable generation of high-quality protein multiple sequence alignments using Clustal Omega. *Molecular Systems Biology* **7**:539. doi: 10.1038/msb.2011.75, PMID: 21988835

Soniat M, Chook YM. 2015. Nuclear localization signals for four distinct karyopherin-β nuclear import systems. *Biochemical Journal* **468**:353–362. doi: 10.1042/BJ20150368, PMID: 26173234

Soniat M, Chook YM. 2016. Karyopherin-β2 recognition of a PY-NLS variant that lacks the Proline-Tyrosine motif. *Structure* **24**:1802–1809. doi: 10.1016/j.str.2016.07.018, PMID: 27618664

Stamatakis A. 2006. RAxML-VI-HPC: maximum likelihood-based phylogenetic analyses with thousands of taxa and mixed models. *Bioinformatics* **22**:2688–2690. doi: 10.1093/bioinformatics/btl446, PMID: 16928733

Susin SA, Lorenzo HK, Zamzami N, Marzo I, Snow BE, Brothers GM, Mangion J, Jacotot E, Costantini P, Loeffler M, Larochette N, Goodlett DR, Aebersold R, Siderovski DP, Penninger JM, Kroemer G. 1999. Molecular characterization of mitochondrial apoptosis-inducing factor. *Nature* **397**:441–446. doi: 10.1038/17135, PMID: 9989411

Süel KE, Gu H, Chook YM. 2008. Modular organization and combinatorial energetics of proline-tyrosine nuclear localization signals. *PLoS Biology* **6**:e137. doi: 10.1371/journal.pbio.0060137, PMID: 18532879

Szczyrba J, Nolte E, Hart M, Döll C, Wach S, Taubert H, Keck B, Kremmer E, Stöhr R, Hartmann A, Wieland W, Wullich B, Grässer FA. 2013. Identification of ZNF217, hnRNP-K, VEGF-A and IPO7 as targets for microRNAs that are downregulated in prostate carcinoma. *International Journal of Cancer* **132**:775–784. doi: 10.1002/ijc.27731, PMID: 22815235

Tagami H, Ray-Gallet D, Almouzni G, Nakatani Y. 2004. Histone H3.1 and H3.3 complexes mediate nucleosome assembly pathways dependent or independent of DNA synthesis. *Cell* **116**:51–61. doi: 10.1016/S0092-8674(03)01064-X, PMID: 14718166

Tao T, Lan J, Lukacs GL, Haché RJ, Kaplan F. 2006. Importin 13 regulates nuclear import of the glucocorticoid receptor in airway epithelial cells. *American Journal of Respiratory Cell and Molecular Biology* **35**:668–680. doi: 10.1165/rcmb.2006-0073OC, PMID: 16809634

Thakar K, Karaca S, Port SA, Urlaub H, Kehlenbach RH. 2013. Identification of CRM1-dependent nuclear export cargos using quantitative mass spectrometry. *Molecular & Cellular Proteomics* **12**:664–678. doi: 10.1074/mcp.M112.024877, PMID: 23242554

Twyffels L, Gueydan C, Kruys V. 2014. Transportin-1 and Transportin-2: protein nuclear import and beyond. *FEBS Letters* **588**:1857–1868. doi: 10.1016/j.febslet.2014.04.023, PMID: 24780099

Visa N, Percipalle P. 2010. Nuclear functions of actin. *Cold Spring Harbor Perspectives in Biology* **2**:a000620. doi: 10.1101/cshperspect.a000620, PMID: 20452941

Vizcaíno JA, Csordas A, del-Toro N, Dianes JA, Griss J, Lavidas I, Mayer G, Perez-Riverol Y, Reisinger F, Ternent T, Xu QW, Wang R, Hermjakob H. 2016. 2016 update of the PRIDE database and its related tools. *Nucleic Acids Research* **44**:D447–D456. doi: 10.1093/nar/gkv1145, PMID: 26527722

von Roretz C, Macri AM, Gallouzi IE. 2011. Transportin 2 regulates apoptosis through the RNA-binding protein HuR. *Journal of Biological Chemistry* **286**:25983–25991. doi: 10.1074/jbc.M110.216184, PMID: 21646354

Wahl MC, Will CL, Lührmann R. 2009. The spliceosome: design principles of a dynamic RNP machine. *Cell* **136**:701–718. doi: 10.1016/j.cell.2009.02.009, PMID: 19239890

Walker P, Doenecke D, Kahle J. 2009. Importin 13 mediates nuclear import of histone fold-containing chromatin accessibility complex heterodimers. *Journal of Biological Chemistry* **284**:11652–11662. doi: 10.1074/jbc.M806820200, PMID: 19218565

Wang P, Liu GH, Wu K, Qu J, Huang B, Zhang X, Zhou X, Gerace L, Chen C. 2009. Repression of classical nuclear export by S-nitrosylation of CRM1. *Journal of Cell Science* **122**:3772–3779. doi: 10.1242/jcs.057026, PMID: 19812309

Weber CM, Henikoff S. 2014. Histone variants: dynamic punctuation in transcription. *Genes & Development* **28**:672–682. doi: 10.1101/gad.238873.114, PMID: 24696452

Weberruss MH, Savulescu AF, Jando J, Bissinger T, Harel A, Glickman MH, Enenkel C. 2013. Blm10 facilitates nuclear import of proteasome core particles. *The EMBO Journal* **32**:2697–2707. doi: 10.1038/emboj.2013.192, PMID: 23982732

Wiśniewski JR, Zougman A, Mann M. 2009. Combination of FASP and StageTip-based fractionation allows in-depth analysis of the hippocampal membrane proteome. *Journal of Proteome Research* **8**:5674–5678. doi: 10.1021/pr900748n, PMID: 19848406

Yoo Y, Wu X, Guan JL. 2007. A novel role of the actin-nucleating Arp2/3 complex in the regulation of RNA polymerase II-dependent transcription. *Journal of Biological Chemistry* **282**:7616–7623. doi: 10.1074/jbc.M607596200, PMID: 17220302

Zhong XY, Wang P, Han J, Rosenfeld MG, Fu XD. 2009. SR proteins in vertical integration of gene expression from transcription to RNA processing to translation. *Molecular Cell* **35**:1–10. doi: 10.1016/j.molcel.2009.06.016, PMID: 19595711

Zhou Z, Licklider LJ, Gygi SP, Reed R. 2002. Comprehensive proteomic analysis of the human spliceosome. *Nature* **419**:182–185. doi: 10.1038/nature01031, PMID: 12226669